LBL-2783
c.2

VAPOR PHASE ETCHING KINETICS OF GaAs

Ronald Henry Bissinger
(M. S. thesis)

June 14, 1974

Prepared for the U. S. Atomic Energy Commission
under Contract W-7405-ENG-48

TWO-WEEK LOAN COPY

This is a Library Circulating Copy which may be borrowed for two weeks. For a personal retention copy, call Tech. Info. Division, Ext. 5545

LAWRENCE BERKELEY LABORATORY
UNIVERSITY OF CALIFORNIA
BERKELEY

LBL-2783
c.2

DISCLAIMER

This document was prepared as an account of work sponsored by the United States Government. While this document is believed to contain correct information, neither the United States Government nor any agency thereof, nor the Regents of the University of California, nor any of their employees, makes any warranty, express or implied, or assumes any legal responsibility for the accuracy, completeness, or usefulness of any information, apparatus, product, or process disclosed, or represents that its use would not infringe privately owned rights. Reference herein to any specific commercial product, process, or service by its trade name, trademark, manufacturer, or otherwise, does not necessarily constitute or imply its endorsement, recommendation, or favoring by the United States Government or any agency thereof, or the Regents of the University of California. The views and opinions of authors expressed herein do not necessarily state or reflect those of the United States Government or any agency thereof or the Regents of the University of California.

PREFACE

The semiconducting compound gallium arsenide is of great importance to the electronics industry. When used to fabricate light emitting diodes (LED's) it is necessary to insure a smooth, damage-free surface on the GaAs wafers. The wafers are generally etched with various solutions or reacted in the gas HCl at high temperatures. The kinetics of the HCl-GaAs reaction are not very well understood. Specifically, the reaction is carried out at atmospheric pressure in a mixture of mainly H_2 with perhaps 10% HCl, and at temperatures from 650° to 750°C. The rates of the commercial vapor etching processes have been empirically determined; however, nothing is known about the surface reaction of HCl with GaAs in the presence of H_2.

It is therefore the purpose of the present study to gain some insight into the GaAs-HCl-H_2 surface reaction and to determine what effect the surface structure has on the reaction.

The main tool used to accomplish this goal was differential gravimetry applied to the GaAs-HCl-H_2 system. Additional aids in the study were derived from existing theory in adsorption kinetics and surface evaporation models. It is hoped that the data and analysis presented in this work will be of some value to the semiconductor processing industry.

LIST OF SYMBOLS

A	area, pre-exponential factor
C	concentration
c	constant
D	diffusion coefficient
E_A	activation energy
F	free energy
H	enthalpy
K	equilibrium constant
k	rate constant, Boltzmann's constant
L	distance between sample and tube wall deposition
M	molecular weight
m	mass of molecule, order of reaction with respect to H_2 (hypothetical)
N	flux
n	order of reaction with respect to HCl
p	pressure
P_r	reaction probability
R	gas constant
r	rate, tube radius
s	step height
T	temperature
V	vacancy
W	work
γ	surface free energy

ε Lennard-Jones constant

θ surface fraction which is covered

ϕ bonding energy

σ Lennard-Jones constant

$\bar{\sigma}$ unit normal to surface

VAPOR PHASE ETCHING KINETICS OF GaAs

Ronald Henry Bissinger

Inorganic Materials Research Division, Lawrence Berkeley Laboratory and
Department of Chemical Engineering; University of California
Berkeley, California

ABSTRACT

Thermal evaporation of (001) GaAs was investigated along with the simultaneous etching by HCl in the presence of H_2. Two kinetic regimes were proposed based on the non-linear Arrhenius plot of the free evaporation rate. In the first regime, at temperatures above 1000°K, the rate exhibited an apparent activation energy of 72 kcal/mole with respect to the HCl; in the second regime, at temperatures below 910°K, an apparent activation energy of 14 kcal/mole was observed.

The gas-solid etching reaction between HCl vapor and solid GaAs was found to have a reaction order of about unity and yielded an apparent activation energy of zero with respect to the HCl. For the overall reaction

$$GaAs_{(s)} + HCl_{(v)} \longrightarrow GaCl_{(v)} + \frac{1}{2} H_{2(v)} + \frac{1}{4} As_4$$

the etching reaction rate can be approximated by

$$r_{HCl} = (9.4\times10^{-6})(p_{HCl})^{1.11}$$

where r_{HCl} has units of mg-cm^{-2}-sec^{-1} and p_{HCl} has units of μmHg and is valid for $930° < T < 980°K$ and $0 < p_{HCl} < 135$ μmHg. A mechanism was proposed in which the rate limiting step is the adsorption of molecular HCl on ledge sites of the GaAs surface.

The addition of H_2 to the vapor phase hindered the HCl etching reaction with GaAs by shifting the dissociated HCl adsorption equilibrium and reducing the adsorbed Cl concentration. The proposed rate limiting step was then the reaction between adsorbed Cl and Ga.

The (001) and (111) planes were found on the etched surface of (001) GaAs, indicating that these were the slowest etching planes. Thermal etching was observed on the (001) and (111) planes. The surface was slightly enriched by gallium after thermal evaporation, suggesting that a liquid gallium layer may form on the surface in the absence of HCl vapor. The subgrain boundaries were preferentially attached by the HCl and were extremely depleted of gallium; the area of these boundaries may amount to 10-20% of the total surface area.

I. INTRODUCTION

Knowledge of the surface reaction in the GaAs-HCl-H_2 is essential to the optimized processing of gallium arsenide wafers in industry. The problem then becomes one of obtaining the surface kinetics of a vapor-solid reaction. The best way of analyzing surface reactions is by combining molecular beam techniques with Low Energy Electron Diffraction (LEED), enabling one to examine even the path of an individual molecule. An alternative approach is to measure the total or overall reaction rate of a macroscopic sample, which includes contributions from both the surface reaction rate and the diffusional resistances offered to the reactants approaching the surface. The researcher has the choice of either determining the diffusional resistances and subtracting these from the overall rate or eliminating diffusion completely from the problem.

Quantifying the diffusional resistance offered to the reactants can be done as in the case of a flow system which overwhelms natural convection caused by differences in density, viscosity, composition and temperature. A well characterized state of forced convection is imposed on the system, as in the hydrodynamic boundary layer adjacent to a rotating disk. Since the properties of the boundary layer are known, the diffusional resistance offered by it to the reactants can then be estimated. Olander[1,2] and

Sparrow and Gregg[3] present the relevant transport equations for the rotating disk case.

Elimination of diffusion completely can be accomplished by the reduction of the total pressure, since gas diffusivities and therefore diffusional resistances vary inversely with the total pressure of the system. By maintaining the total pressure below 1 torr it is possible to minimize or remove diffusional resistances. This has been done for the graphite-oxygen system by Rosner[4] and Blyholder.[5]

The first method of determining the diffusional resistance has been used by Goettler[6] in the chloride transport vapor deposition of GaAs. He modeled the surface reaction as being driven by a chemical potential force which was then combined in series with diffusion of the reactants through a stagnant film. A laminar jet of reactant gas was directed normal to the surface of the substrate in order to minimize the diffusion effects and to permit the calculation of the diffusional contributions. His results suggested a transition in the surface kinetics in the temperature range of 700-750°C.

The second technique, elimination of the diffusional resistances completely, is utilized in the present study. It is relatively simple to use the weight change of a sample to follow the reaction rate. Microbalances have

been used by several researchers to obtain rate data in a manner similar to the one employed in this work.

Shaw[7] has used a Cahn electrobalance to study the epitaxial growth of GaAs on GaAs substrates of (001) orientation. Activation energies of 48.7±3.5 kcal/mole were found for the kinetically controlled region; i.e., temperatures below 750°C. A "quasiequilibrium" model, originally developed by Sedgwick[8] for silicon epitaxy, was applied and found to agree well with the observations at low GaCl and As_4 partial pressures and high temperatures.

Lou[9] has investigated the vaporization mechanism of GaAs single crystals by using a sample suspended from a microbalance at 10^{-7} torr and from 650° to 900°C. She found that GaAs decomposed into gaseous As_2 and As_4, and a liquid film of gallium. Coupling of a mass spectrometer to the system showed that the (111) or the Ga face produced only As_4 while the $(\bar{1}\bar{1}\bar{1})$ or As face yielded both As_2 and As_4 vapors in the ratio of 3:1.

Rosner and Allendorf[4] have investigated the reaction between pyrolytic and isotropic graphite and oxygen using a total system pressure of 1 torr and an oxygen partial pressure of 3×10^{-2} torr. A constant activation energy was departed from on several occasions, presumably due to a change in the surface kinetics.

Blyholder and Eyring[5] have done similar work for the graphite-oxygen system at temperatures from 600° to 1300°C and from 1 to 100 μmHg pressure. They found the surface reaction to be dependent on impurities in the graphite and surface porosity.

It is clear that while the technique of differential gravimetry has been applied previously and is fairly well documented, it's application to GaAs etching by HCl in the presence of H_2 represents a new extension. The work done in the cited references will serve to establish an experimental technique framework in which to perform the present study.

Differential gravimetry is used in the present study to determine the evaporation mechanism of GaAs and how that mechanism is affected by HCl and H_2. In addition, a rate equation for GaAs-HCl reaction is presented, and the macroscopic and microscopic surface of the GaAs is examined in relation to evaporative and reactive conditions. The examination of the GaAs reaction with HCl and H_2 is unique, and the results described herein are valuable to the optimization of the etching and deposition reactions of GaAs and other III-V compounds as well.

II. THEORY

A. Introduction

The problem with developing a suitable model for the GaAs-HCl-H_2 reaction is that there is really no comprehensive understanding of how a binary vapor phase will react with the crystal surface. The possible surface mechanisms are numerous and the specification of a probable mechanism is subject to confirmation by more direct methods. Similarly, the surface model which has been previously developed is limited to monatomic solids freely evaporating into a vacuum. The present system involves the dissociating solid GaAs reacting with a vapor phase, in addition to thermally evaporating. Development of a detailed model for the present case is well beyond the scope of the present work; instead, an effort will be made to extend the existing theory for monatomic free evaporation to a dissociating surface undergoing chemical reaction. The result will be a semi-quantitative understanding of the GaAs-HCl-H_2 reaction.

The problem can be broken down into three main areas: the surface of GaAs, surface reaction kinetics, and the theory of evaporation. The surface of GaAs essentially constrains the mechanism and hence the observed reaction rate. The various models of evaporation provide a basis for interpreting surface adsorption phenomena for this system, which in turn will be linked to the overall rate. The

emphasis will be on extending, when justified, the existing theory to the GaAs-HCl-H_2 system.

B. Crystal and Surface Structure of GaAs

It is well known that the reaction rate between a crystal and a vapor may depend on the orientation of the crystal. The reasons for the phenomenon are surface stoichiometry, surface packing, surface free energy, and surface planarity. It is useful to begin by describing the crystal structure of GaAs.

The compound gallium arsenide has the zinc blende structure with a lattice parameter of 5.653Å. The unit cell and tetrahedral bonding are shown in Fig. 1. The gallium atoms are located on an FCC sublattice centered at the origin (0,0,0), while the As atoms are located on an FCC sublattice centered at $(\frac{1}{4},\frac{1}{4},\frac{1}{4})$. The bonding structure of the (001) surface is shown in Fig. 2.

The GaAs samples used in this experiment were cut so that the surface normal was displaced 2° from the [001] in the (110) plane. This is shown in Fig. 3.

Examination of Figs. 1 and 2 show that alternate (001) planes are of either Ga or As; these planes are equally spaced at one-quarter of the lattice parameter. Since each atom has four bonds it is seen that those atoms on the (001) surface plane will have two unsatisfied bonds. These bonds determine the surface free energy, which will greatly

affect the growth and etching rates of the (001) surface. Sangster[10] provides a convenient summary of growth rate and crystal orientation relationships for GaAs. Under growth conditions the (001) surface has very good nucleation characteristics, poor surface stoichiometry, fair surface packing and very poor surface planarity. Sangster also predicts that the fastest growth direction for a (100) surface will be the ⟨311⟩ since it is a compromise between the good and the poor characteristics of the ⟨100⟩ and the ⟨111⟩ directions. Likewise, it should be expected that for the (001) surface growth, and etching, will proceed fastest in a direction other than the ⟨001⟩; in particular, following Sangster's reasoning, for a (001) orientation the fastest growth direction should be the ⟨113⟩ . The vicinal (113) surface will be composed of (001) and (111) steps.

One can generalize these results in terms of the surface free energies. For solids the surface free energy γ is equal to the surface tension if no species are adsorbed. γ is defined as the reversible work dW needed to create a unit surface area dA by separation at constant temperature, constant volume, and constant chemical potential,

$$\gamma = \frac{dW}{dA} \qquad (1)$$

If $\bar{\sigma}$ is the unit normal to a crystal plane, and if the volume is constant, then the equilibrium shape will be that shape which minimizes the quantity γA; i.e.,

$$\int \gamma(\bar{\sigma})dA \quad \text{is minimized} \tag{2}$$

A plot of γ as a function of orientation known as Wulff of polar γ plot, can be used to construct an equilibrium shape of the crystal.[11,12] In the present study of GaAs the reaction is carried out far from equilibrium, and it is possible that the equilibrium shape can never be achieved. It has been shown that the surface free energy is significant only when the size of the crystal is small, approximately one micron or less. If the crystal is any larger then temperature gradients, anisotropic kinetics, and other driving forces large enough to cause measureable reaction rates will completely overwhelm surface free energy constraints.[11,13] This evidence is not sufficient to rule out the formation of an equilibrium crystal shape. For etching and evaporation, the fastest etching planes should disappear first, leaving the slowest etching planes behind. As already pointed out, the surface free energy is only one factor which determines the reaction rates of a particular plane. For GaAs the (001) plane has a higher free energy than the (111), therefore one would expect the surface to be composed of mostly (111) faces with some (001) surfaces, if the surface free energy is a constraint in this particular case.

It is also possible that while a minimized $\int \gamma(\bar{\sigma})dA$ will not determine the overall crystal shape, it will affect the surface to some degree. This is manifested by thermal faceting, a spontaneous creation of fine ridges in a surface. The facets are actually made of low index and complex planes. A detailed explanation of the facet width dependency on time, along with a summary of related work, is given by Moore.[14]

C. Surface Reaction Kinetics

1. Equilibria

It is useful here to begin with a description of the stoichiometry of the GaAs-HCl-H_2 reaction. Ban[15] has confirmed the equilibrium reaction:

$$GaAs_{(s)} + HCl_{(g)} \rightleftharpoons GaCl_{(g)} + \frac{1}{4} As_{4(g)} + \frac{1}{2} H_{2(s)} \qquad (3)$$

as the one occurring during the deposition of GaAs by the chloride transport process. The equilibrium constant is given by

$$K_{eq} = \frac{p_{GaCl} \cdot p_{As_4} \cdot p_{H_2}^{1/2}}{p_{HCl}} \qquad (4)$$

Kirwan[11] summarizes the relevant equilibria for the Ga-H-Cl-As-P system; specifically he gives K_{eq} as

$$\log_{Lo} K_{eq} = [-8.04 + \frac{6.99\times10^{3}}{T} + 0.22\ \ell nT + \frac{0.35\times10^{-3}}{T}]^{-1} \quad (5)$$

Equation 5 is valid for 300°K < T < 2000°K.

2. Reaction Activation Energy and Order

If it is assumed that hydrogen can participate in the reaction between GaAs and HCl, then the overall rate may be expressed as

$$r = Ae^{-E_A/RT}\ p_{HCl}^{n}\ p_{H_2}^{m} \quad (6)$$

over a limited range of temperature and pressure. In this situation the activation energy E_A is a linear combination of the individual activation energies of the elementary steps.

At the temperatures used (T > 600°C) the GaAs was continuously dissociating into Ga and As species, the rate of which is called r_{THERM}, the thermal evaporation rate. It is assumed that the reaction reaction rate due to the HCl, r_{HCl}, is superimposed upon the thermal evaporation rate; in other words, r_{THERM} is unaffected by the addition of HCl. This is a very bold assumption, and more likely than not invalid for precise analysis. In most cases the adsorption of a gas on the surface of an evaporating solid will affect the evaporation rate, usually increasing it. However, it is impossible at present to determine how the

HCl perturbs the thermal evaporation rate, and the assumption that $r_{THERM} \neq f(p_{HCl})$ is used. HCl was bled into the system and the difference between the total rate, r_{TOT}, and the thermal evaporation rate, r_{THERM}, is the rate due to HCl only, r_{HCl}. A plot of log r_{HCl} versus log p_{HCl} will give a straight line, the slope of which is the order of reaction with respect to HCl, n.

When both HCl and H_2 are in the vapor phase, it is not possible to separate r_{HCl} from the influence due to hydrogen; it is prevented by the imprecision of the data. Instead, it is proposed that the rates be combined, so that $r_{HCl,\,H_2} = (r_{TOT} - r_{THERM})$. In this way r_{HCl} measured with no H_2 present can be compared with the r_{HCl} measured with H_2 in the vapor phase. Again, it is assumed that the thermal evaporation rate is not affected by either HCl or H_2. The combined rate $r_{HCl,\,H_2} = r_C$ can be assumed to be of the form

$$r_{HCl,H_2} = kp_{HCl}^{n}p_{H_2}^{m} = r_C \qquad (7)$$

with $k,n,m \neq f(p_{H_2}, p_{HCl})$. Taking the natural log of both sides and the partial derivative with respect to ln p_{HCl} results in

$$\left(\frac{\partial[\ln(r_{H_2} + r_{HCl})]}{\partial[\ln p_{HCl}]}\right)_{p_{H_2}} = n \qquad (8)$$

Similarly,

$$\left(\frac{\partial[\ln(r_{H_2} + r_{HCl})]}{\partial[\ln p_{H_2}]}\right)_{p_{HCl}} = m \qquad (9)$$

It is seen that if r_{HCl,H_2} is plotted versus p_{H_2} and p_{HCl} the orders of reaction m and n are obtained respectively from the slopes. In this manner the effect of hydrogen on the reaction is clearly seen.

3. Surface Reactions and Adsorption

Most surface reactions involve an adsorbed species on the surface, whether it be an adsorbed vapor phase atom or an adsorbed atom the same as the solid. In evaporation there is no difference between the two types (if the vapor consists of the same substance as the solid). A brief description of the various surface mechanism possibilities and related adsorption phenomena is in order at this point.

The process of ideal surface adsorption is modeled by Langmuir's adsorption isotherm in which nondissociated gas molecules (or atoms) fill single sites on the surface. The rate of adsorption r_a is given by

$$r_a = k_a p(1-\theta) \qquad (10)$$

with k_a the adsorption constant. From this can be derived

the Langmuir equation

$$\theta = \frac{Kp}{1+Kp} \tag{11}$$

In certain cases a molecule may dissociate upon adsorbing on the surface, which is depicted as follows:

$$HCl + \begin{array}{c} | \quad | \\ -S-S- \end{array} \rightleftharpoons \begin{array}{c} H \quad Cl \\ | \quad | \\ -S-S- \end{array} \tag{12}$$

where HCl is a vapor phase molecule and $\overset{|}{-S-}$ are available surface adsorption sites. The surface sites are not the same, since both Ga and As atoms have different ionic bond characters. For example, each site may have two unshared bonds that could be used for adsorption. The rate of adsorption for dissociating HCl is

$$r_a = k_a \, p(1-\theta_H-\theta_{Cl})^2 \tag{13}$$

Conversely, the rate of desorption is

$$r_d = k_{-a} \, \theta_H \theta_{Cl} \tag{14}$$

When two different species compete for the surface sites the results are different. If A is one component and B the other, and adsorption requires only one surface site, then the respective fractions of the surface covered are given by

$$\theta_A = \frac{K_A p_A}{1 + K_A p_A + K_B p_B} \tag{15}$$

and

$$\theta_B = \frac{K_B p_B}{1 + K_A p_A + K_B p_B} \tag{16}$$

Note that as the pressure of one gas is increased the fraction of the other gas's coverage decreases. This is related to the rate of reaction, since the driving force for the surface reaction can be the quantity of adsorbed material available for reaction.

The degree of adsorption in a reaction depends on the mechanism. There are two main types of surface reactions which occur: the bimolecular surface type, and the Langmuir-Rideal type.

The bimolecular surface mechanism requires the adsorption of the reactants on the surface, after which the chemical reaction takes place. It can be described as the following:

$$Ga_{(a)} + Cl_{(a)} \longrightarrow GaCl_{(a)} \tag{17}$$

In this particular instance the rate of reaction may be written as

$$r = k\,\theta_{Cl}\theta_{Ga} \tag{18}$$

The Langmuir-Rideal mechanism requires that only one reactant be adsorbed on the surface. If Ga is adsorbed on the surface and Cl is in the vapor phase, then the reaction will be as follows:

$$Ga_{(a)} + HCl_{(v)} \longrightarrow H_{(v)} + GaCl_{(v)} \qquad (19)$$

The rate for this step may be expressed as $r = kp_{HCl}\theta_{Ga}$.

It is possible, in a bimolecular surface reaction, for the rate to attain a maximum as the reactant partial pressure is varied. This occurs by maximizing the number of adjacent reactant sites; this behavior is illustrated in Fig. 4. Note that a Langmuir-Rideal mechanism does not exhibit a maximum rate.

It is possible at this point to suggest the most probable reaction mechanisms between GaAs and HCl. But the fact that GaAs is a crystal implies that the arrangement of atoms on the surface, and hence surface reactivity, might be modeled. In particular, the process of evaporation has been modeled for crystal surfaces, and it is now attempted to extend this evaporation theory to include the chemical reaction on the surface as well. It is best, then, to

postpone the presentation of possible mechanisms until the surface model is developed.

4. The Surface Reaction and Evaporation Model

Since the chemical reaction of GaAs with HCl is in series with the free evaporation of GaAs, some basic theory for the evaporation process will be described initially; then the complication of a surface reaction will be involved.

If a monatomic single crystal of Ga is allowed to evaporate into a vacuum (free evaporation) according to the reaction $Ga_{(s)} \rightarrow Ga_{(v)}$, then the flux N_v of the vapor species from a stable face is:[16]

$$N_v = k_v C_s \tag{20}$$

where k_v is the rate constant for the rate limiting step, and C_s is the surface concentration of Ga atoms in the rate limiting step. If the solid is in equilibrium with its vapor the rate of evaporation will equal the rate of condensation; this condition may be expressed by elementary kinetic theory,[17] but is meaningless here since the vapor-solid equilibria can never be attained. Somorjai and Lester[17] point out the deficiencies in assuming equilibrium equations apply to nonequilibrium situations, such as the free evaporation of GaAs. The mechanism for equilibrium evaporation of GaAs is not necessarily the same as for the nonequilibrium evaporation.

Somorjai and Lester[17] investigated the dissociation of CdS single crystals using stoichiometry measurements, photoactivation, and by evaluating impurity effects. For both GaAs and CdS the activation enthalpy $\Delta H^{\ddagger}$ of the transition complex was less than the heat of vaporization ΔH_v. These results imply that the rate limiting step is not the desorption of surface atoms but either the surface reaction itself, surface diffusion, or the dissociation of the compounds on the surface.

On the molecular level the process of evaporation can be modeled by the Terrace-Ledge-Kink (TLK) model. If a low index plane is considered as in Fig. 5, and the surface is atomically flat or singular, then surfaces close to the low index plane are broken down into terraces and steps, which is a so-called vicinal surface. If the angle θ of deviation of the surface normal from a low index direction is small, such that $\tan \theta \ll 1$, the steps have a height s and a density of θ/s. For the case of (001) GaAs with the surface normal angled 2° along the (110) plane, the length of the terraces (from step to step) is 40.47Å, and s is equal to one-quarter the lattice parameter, 1.41Å.

Figure 5 also shows surface atoms in several characteristic positions. An atom in position B, an adatom, would seem to be the most likely to desorb (evaporate) or react, since it is the least strongly bound to the crystal. An atom

in position D appears to be the least likely to desorb or react, since it is the most strongly bound position. The tendency to desorb in terms of position can be written B > A > C > D.

According to the TLK model, it is assumed that there is an equilibrium between atoms at the ledge and kink positions, positions A and C respectively in Fig. 5, which reflects a rapid surface diffusion. Evaporation of GaAs might then occur by the following steps:[17]

$$\text{ledge atoms} \underset{k_2}{\overset{k_1}{\rightleftharpoons}} \text{adsorbed atoms (position B)} \quad (21)$$

$$\text{adsorbed atoms} \underset{k_4}{\overset{k_3}{\rightleftharpoons}} \text{vapor phase atoms} \quad (22)$$

$$\text{ledge atoms} \underset{k_6}{\overset{k_5}{\rightleftharpoons}} \text{vapor phase atoms} \quad (23)$$

Ledge atoms diffuse across the surface in a perpendicular direction away from the ledges, and are then considered adsorbed atoms. Table 1 gives the free energies for steps 21-23 for crystals of various orientations.

It is possible to determine k_i for values of i equal to 1,2,3, and 5. Somorjai and Lester[17] state that $k_i = \nu \exp(-\Delta F_i/kT)$ for i=1,2,3,5; ν is the vibrational frequency of the surface atoms (about 10^{13} sec^{-1}), and ΔF_i is the free energy change of the reaction. However, there

is some question of the validity of applying these expressions to a dissociating solid such as GaAs. Certainly these values will not reflect k_i for a substance other than GaAs, such as HCl or H_2, which adsorbs on the surface. Rough order of magnitude values of k_i for i=1, 3,5 are presented in Table 2 for GaAs, assuming ΔF_i values from Table 1. For i = 4,6, the expressions are dependent on the vapor phase concentrations, and it is possible to assume that for Ga and As, step 4 and step 6 is zero for dissociation into a vacuum.

Step 5 has a high activation energy (k_i, $k_3 > k_5$) and so step 5 can also be assumed negligible. The overall rate of vaporization is then controlled by the production rate of adatoms; this production is, in turn, controlled by the surface diffusion from ledge sites. Therefore the entire process is diffusion controlled.

Hirth and Pound[18] analyze the surface concentrations of adatoms on the surface (terraces and ledges) of a monatomic solid undergoing evaporation. Expressions for the concentration gradients and the mean spacing between ledges are presented. In the case of GaAs evaporation and reaction, the expressions contain the surface concentration of adatoms as functions of distance from the ledges, and equilibrium partial pressures; both quantities are indeterminate for the present case, and hence the analysis cannot be used here.

A study of surface diffusion is presented by Gjostein,[19] in which the author presents a generalized expression for the surface diffusion coefficient D_s for a TLK surface. Again the expression is rendered indeterminate when the dissociation of GaAs, the adsorption of HCl and H_2, and unequivalent sites are considered.

Arthur[20] has used the TLK model to calculate Zn desorption fluxes from GaAs surfaces, which agreed well with the experimental data. He found that Zn bonded with As on the surface to form nucleation sites for further Zn adatoms. Zn would diffuse across the surface until it contacted the zinc "islands", at which time it would join with the island boundary. The zinc was assumed to adsorb on the ledge and kink sites, and was verified by the experimental results. Arthur also pointed out the contamination difficulties of carbon and oxygen on the GaAs surfaces.

The TLK model assumes the surface is free; i.e., there is no film of liquid gallium on the surface. Lou[9] found evidence that the surface was indeed covered by such a film, but her experiments were done at temperatures of about 850°C as compared with the 735°C of the present studies. If a liquid Ga layer did form the TLK model would be invalid. The data indicates that Ga did accumulate on the surface during thermal evaporation, but that the HCl removed it as quickly as it formed. Therefore the TLK model

can be applied to the HCl etching situation, but not to pure thermal evaporation.

5. Possible Reaction Mechanisms

As mentioned before, there are two types of reaction mechanisms that are possible: the bimolecular surface and the Langmuir-Rideal mechanisms. The essential difference is that the former requires the adsorption of HCl on the surface prior to reaction, whereas the latter states that the HCl reacts directly from the vapor phase.

For the case of evaporation Lou[9] has proposed a mechanism for the evaporation of (111) GaAs single crystals based on the information provided by mass spectrometric observations. The mechanism can apply to (001) GaAs as well if there is provision made for the crystal surface being homogeneous as compared to the (111)A and (111)B faces of (111) GaAs crystals. Lou proposed a suitable basic mechanism and is reporduced in Table 4a. The rate limiting step is postulated to be the formation of the surface divacancy $[V_{Ga}V_{As}]$, which is the sum of the first three steps given in Table 4a. There is no reason why this formation sequence would not limit the evaporation rate of (001) GaAs also.

By examining other reactions similar to the one between HCl and GaAs it is possible to speculate on the mechanism of the GaAs etching. One such study involved the reaction between molecular chlorine and germanium and silicon surfaces,

done by Madix and Schwarz.[21] In this study a modulated molecular beam was coupled with mass spectrometric phase-sensitive detection to find that at above 850°K the germanium reaction was first order, as was the silicon reaction above 1050°K. The rate limiting step was hypothesized to be the adsorption of molecular chlorine on the surface of the compound. First order behavior was also found for the molecular bromine reaction with germanium,[22] and the surface diffusion of an intermediate was the rate determining step.

Madix et al.[23] found a low reaction probability of about 0.01 for oxygen reacting with germanium, which was due to the steric hinderance of the dissociation of the O_2. The adsorption of reactants and product desorption limited the reaction in different regimes. Reaction probabilities of 0.2-0.5 between room temperature ozone and (111) germanium were found at ozone pressures of about 5×10^{-6} torr, and at surface temperatures of 800°K.

It is possible to have the HCl react at either the terrace or ledge positions. Table 3 presents the possible surface mechanisms divided into three categories: Ledge, Terrace, and Rideal mechanisms. The confirmation of any one sequence by the experimental data should be viewed as a confirmation of the most prevalent reaction; i.e., the specified mechanism is the fastest, and hence influences the overall kinetics the most.

III. EXPERIMENTAL

A. Apparatus

In order to investigate the surface reaction of HCl and H_2 on GaAs a reactor had to be designed which would provide a constant temperature, a vacuum below 1 μmHg, and a fine metering capability for the reactant gases. In addition, the weight of the sample would have to be continually monitored. Such a system is shown in Fig. 6.

The heart of the apparatus is a Perkin-Elmer AR-1 Autobalance with a 5 gram capacity. The microbalance weighing unit is housed in a glass enclosure which has a provision for passing a purge gas through the system. One port of the enclosure contains the taring or counterweighing pan while the other port connects directly to the reactor enclosure. The suspension fibers are made of quartz, either 0.508 or 0.127 mm in diameter. The microbalance output is fed to a 10 mV recorder with variable chart speed and offset voltage.

The sample and part of the suspension fiber is housed in the reactor tube, 50 mm I.D., 86.5 cm long, and made of quartz. The tube is sealed at both ends by O-ring type endcaps made of 316 stainless steel. The endcaps and the section of the reactor tube between the endcaps and the furnace housing are water cooled to protect the Viton O-rings. The top endcap has a $\frac{1}{4}$-inch feedthrough for a

thermocouple well, another 1/4-inch feedthrough for the HCl stainless steel inlet tube, an 11 mm feedthrough for the pressure sensors, and a 3/8-inch O.D. centered tube through which the sample suspension fiber passes through to the reaction zone. The bottom endcap is similar except there are three 1/4-inch feedthroughs for the three thermocouples, and a 3/8-inch outlet for evacuation.

The vacuum exhaust line is made of 3/8-inch O.D. stainless steel with 1/4-inch isolation valves. Between the system and the 2-inch diffusion pump are two pyrex cold traps filled with liquid nitrogen. The traps serve the dual role of preventing HCl from reaching the pumps and preventing pump oil from reaching the reactor tube.

The pressure is monitored by a McCleod gage and a thermocouple gage connected to the 11 mm tube passing through the top endcap. A second thermocouple gage was placed between the cold traps and the diffusion pump. A vent placed in the line before the diffusion pump enabled the system and traps to be purged with argon before and after the runs.

The HCl is 99.99% pure, electronic grade. The H_2 is passed through a deoxo unit and then liquid nitrogen cold trapped. The argon purge gas is passed through a titanium-bed gettering furnace and cold trapped with trichloroethylene and dry ice. The gases are metered through Nupro double-pattern needle valves and shut off is obtained by bellows on-off valves. The gases could be metered with the Gilmont

micro-flowmeters but this proved to be unreliable and the flowmeters are used for visual checks only. All gas lines, valves, and fittings are 316 stainless steel Nupro, Cajon Ultra-Torr, and Swagelok brands.

A resistance type-furnace surrounds the main quartz tube. The furnace is a clamshell design and can attain 1100°C at the center. A typical temperature profile is shown in Fig. 8, although a great many profiles are available because the furnace has three independent zones. Each zone has its own proportional temperature controller which, over a period of six hours, maintains the desired temperature to ± 1°C. Each zone is controlled through a chromel-alumel (type K) thermocouple which is read by a Leeds and Northrup potentiometer. A separate thermocouple is located approximately 1/4-inch below the sample and is connected to a recorder as a continuous monitor. A fifth thermocouple is placed between the furnace and the wall of the quartz reactor tube to insure that the temperature do not exceed 1100°C, roughly the annealing point of quartz. The thermocouple is fed into an alumina sheath and the four thermocouples on the inside of the reactor tube are placed in quartz tubes to insure airtightness and inertness.

The system also has the capability of depositing epitaxial layers and investigating surface kinetics by the rotating disk technique. Since safety is an important consideration when working with III-V compounds, everything except the electronics and gas purification systems was enclosed in a special fume hood.

The loading of the sample is an extremely delicate procedure. The microbalance enclosure has to be moved horizontally to allow the suspended sample to be lowered into the reactor tube. The coupling section between the top endcap and the microbalance enclosure also is an evacuated dewar designed to condense any potentially harmful vapors before they can reach the microbalance weighing mechanism. This is judged unnecessary because of the low pressures involved and the inherent corrosion resistance of the microbalance mechanism itself. However, when H_2 is used the H_2 is added to the system through the microbalance enclosure and hence served as a purge gas stream.

It should be noted that there is an important design criteria which relates the diameter of the reactor tube to the pressure required to do reliable free evaporation studies. Since it is desired to avoid the back reflection of product molecules from the tube walls (which would mean there is a net flux of material to the sample surface), the mean free path at the operating conditions should exceed a

characteristic dimension of the system; namely, one-half the diameter of the tube. Appendix A illustrates the mean free path calculation for HCl (useful for etching studies) which shows that the mean free path at 10 μmHg pressure and about 1,000°K is about the same as the tube radius. Since GaCl, As_2, and As_4 will be slightly different in mass than HCl, the mean free paths will differ for each species, but essentially there will be little reflection from the tube walls regardless of the product. In other words, diffusional resistances are zero. Although the operating pressures run almost to 200 μmHg during the etch reactions it is safe to assume that the diffusional resistances are also negligible here.

B. Sample Preparation

The GaAs samples are obtained* cut in the (001) plane with the surface normal angled 2° along the (110) plane (see Fig. 3). The specimens have one side highly polished and the other side have a lapped finish.

In order to minimize the surface damage that polishing inflicts on the samples, a chemical etch is used. A solution of 3:1:1 H_2SO_4:H_2O_2:H_2O, cooled to room temperature and continuously stirred provides an excellent etchant for GaAs wafers. The samples are etched in the solution

---

*- Monsanto, St. Louis, Missouri

for 15 minutes, rinsed with deionized water, and air dried. Both sides appear semiglossy at this point, although one side is somewhat shinier. The mechanical damage done by cutting and lapping has been removed. Before insertion into the apparatus the samples are washed in trichloroethylene, rinsed with acetone, washed again with isopropanol and blown dry. In this manner all organic contaminants can be removed.

Before and after reaction the samples are photocopied against a standard cross-section to determine the surface areas. The areas are measured by polar planimeter, and adjusted for distortion error in the copying process.

The samples are also weighed on a Mettler balance before and after the run to provide a standard weight for the microbalance calibration procedure.

C. Operating Procedure

The samples are placed in the sample holder, a wishbone-shaped quartz fiber that provides a spring tension on the sample to prevent slippage. The system is assembled, evacuated, and checked for leaks. When the system is tight it is then backfilled with argon and purged with the gas, sixty minutes for the first run and ninety minutes for the second. Two runs were performed, the first with HCl only, the second with both HCl and H_2. The HCl and H_2 lines are

flushed with their respective gases during this purge period. The entire system is then sealed and evacuated for twenty to twenty four hours. During the last eight hours of this evacuation period the reactor tube and the sample are baked out at about 340°C. The temperature is then increased to the desired final temperature, with the temperature being increased from the bottom zone to the top zone in order to minimize temperature control fluctuations.

The first piece of data obtained is the free evacuation rate, r_{THERM}, with no gas present in the reactor. A reactant gas, either HCl or H_2, is metered in and the pressure is allowed to reach a steady state, usually in about twenty minutes. The temperature and pressure are noted, and then the gas flow rate is varied, hence the pressure is changed. If both gases are used simultaneously, the HCl is first metered in, allowed to stabilize, and then the H_2 is added, with the resulting difference in pressure considered to be the partial pressure of H_2. This procedure is repeated at a given temperature until the desired data is obtained. The temperature is then changed and the procedure repeated again.

After the run is completed the gas flows are shut off and the system is allowed to pump down as it cools. Once the sample reaches room temperature the pumps are sealed off and the rest of the system pressurized and purged with argon for twelve hours. The sample is then removed and analyzed.

IV. RESULTS

The data obtained yielded information for the free evaporation rate of GaAs, the surface reaction with only HCl, the surface reaction with HCl in the presence of H_2, and to some degree the surface morphology of the samples. The results will then be broken down into these sections.

A. Free Evaporation of GaAs

Free evaporation rates were obtained when the pressure in the reactor tube was 8 μmHg or less. It is assumed that under these conditions there was no reactive gas in the system. Appendix B is a complete listing of operating conditions for each data point and will be useful for relating the data point numbers used in the rest of this study to the experimental conditions. Of the 63 data points listed, the ones for free evaporation analysis are shown in Fig. 9 as an Arrhenius plot of rate versus 1/T. It is apparent that two rate controlling steps compete in the temperature range studied. The high temperature asymptote yields an activation energy for the transition state of 72 kcal/mole, while the low temperature asymptote yields about 14 kcal/mole. These figures are not precise, since inspection of Fig. 9 shows that the temperature range is not sufficiently broad to give two distinct, straight lines at either end of the temperature range. It is likely that

the high temperature value for ΔH^* will increase, and that the low temperature value will decrease if the experiment was run at higher and lower temperatures. The dashed line to the left of the data points in Fig. 9 is an extrapolation from Lou's data[9] for the vaporization of (111) GaAs single crystals into a vacuum. It is seen that Lou's observed $\Delta H^{\ddagger}$ value of 90 kcal/mole is similar to the value obtained in this study. Her experiments were done at too high a temperature to observe any change in the kinetics. The data points with asterisks in Fig. 9 were obtained in the presence of H_2 only, shown here as a comparison to the pure evaporation case. More will be said about these points in the discussion section.

B. Pure HCl Reaction with GaAs

As previously discussed in the theory section, the difference between the total reaction rate and the thermal rate is assumed to be the rate due to the HCl reaction, r_{HCl}, when only HCl is present. Figure 10 is a plot of $\ln r_{HCl}$ versus $\ln p_{HCl}$ for four different temperatures. Least squares was used to determine the slopes, which are the order of reaction n with respect to HCl. The value of n varies from 0.96 to 1.45, and the rate constant k varies from 1.9×10^{-6} to 1.4×10^{-5}. There does not appear to be any clear temperature dependence the rate constant k, but n decreases with increasing temperature.

Figure 11 is the same plot as Fig. 10 except that Fig. 11 is for one temperature, 736°C, and illustrates an apparent time dependency of the order of reaction. Since the numbering of the data points increases with time, Fig. 11 indicates a definite trend for the order to decrease from it's high value of Line 2-3 to a lower value of Line 5-6, which approaches closely the orders obtained in Fig. 10. The solid line in Fig. 11 is a least squares fit for all the points shown, and yields an order of 2.45 with a rate constant k of 5.4×10^{-9}. Note that in both Figs. 10 and 11 there is no tendency for r_{HCl} to approach a limit as p_{HCl} increases, and is expected.

C. HCl Reaction with GaAs with H_2 Present

Since it is impossible to differentiate directly the individual rates due to HCl and H_2, the two rates are combined as the difference between the total rate and the thermal rate. Figure 12 is a plot of the natural log of the combined rate $r_{HCl,H_2} = (r_{TOT} - r_{THERM})$ versus the natural log of p_{H_2} for three ranges of relatively constant p_{HCl}. Note that one curve increases with increasing p_{H_2}, but it will be shown that this curve is erroneous. The other two curves have a zero slope (or nearly so) for low p_{H_2}, hence the order of reaction with respect to H_2 can be considered zero (m=0). But for large p_{H_2} the slope becomes negative,

and m becomes negative, indicating that the H_2 is somehow hindering the reaction. A comparison of the two lines in Fig. 12 shows that the combined rate is higher for large p_{HCl} (39±1μmHg) than for lower p_{HCl}(17±1μmHg), and yet for low p_{H_2} both orders of reaction are zero. The same phenomenon is observed in Fig. 13, which is the same as Fig. 12 except for a different temperature and different p_{HCl} ranges.

The combined rate can be plotted versus p_{HCl} to determine the dependency of the rate on the partial pressure of HCl. In Figs. 14 and 15 the natural log of the combined rate (r_{TOT} - r_{THERM}) is plotted against the natural log of p_{HCl} for different temperatures and H_2 partial pressures. The curves are shown to pass through maxima, although it can be argued that they should be drawn as straight lines. But it is highly unlikely that random error can occur four times in the same pattern, as would be required in this instance. Because of such an improbability, the curves are drawn as in Figs. 14 and 15. It is obvious that at 686°C the curves are higher than for 630°C, since the reaction of the GaAs with the HCl would be expected to increase with increasing temperature. The curvature is less prominent in the corresponding linear plots shown in Figs. 16 and 17.

When the rate constants, k, are corrected for a unity order and plotted versus 1/T, the slopes are zero. This zero activation energy is found both for the pure HCl reaction and the reaction with both HCl and H_2 present in the vapor phase, and will be explained in the discussion section.

D. Surface Morphology of GaAs

Visual inspection showed that the surface of sample #1 was slightly rougher than before the reaction, and that both sides appeared to be identical. The surface of sample #2 was extremely rough with both sides being the same. Appendix B, Table A gives a comparison between sample #1 (run #1) and sample #2 (run #2).

The surfaces were further examined using a scanning electron microscope (SEM). An unreacted sample which had been chemically etched the same as the two reacted specimens was used as a reference. At 10,000 magnification the shiny side of the reference was absolutely smooth, while the slightly rougher side appeared to be just barely roughened.

It is believed that this initial discrepancy disappeared during the first few minutes of thermal etch.

Figure 19 is an SEM photograph of sample #1 from the first run etched in HCl only. At the 2,000 magnification the surface is relatively smooth although considerably rougher than the reference. Thermal etch pits are present, with white material surrounding some of them. Sample #1 was thermally equilibrated, after etching, at 663°C before quenching.

Figure 20 is an SEM photograph of sample #2 from the second run in HCl and H_2, shown at a magnification of 500 diameters. Thermally equilibrated at 736°C before quenching, the sample is extremely rough with faceted hillocks. Thermal faceting ridges are noticable on the sides of the hillocks. The facet sides are (111) planes while the floors are (001) planes.

Figure 21 is an enlargement of an area above the center of Fig. 20. At 2,000 magnification the difference in structure of the surface on either side of the ridge is evident. The lower side is an example of a vicinal surface where the overall (111) plane is composed of many steps and ledges of other orientations. Thermal faceting is also apparent.

Figure 22 is a 2,000 magnification photograph of a peak below and left of the center of Fig. 22, which exhibits thermal faceting and a large (111) flat in the lower right hand corner.

Another area of sample #2 is shown in Fig. 23 at 300 diameters. Note the large (001) flats, the (111) sloping sides, and the thermally etched ridges. The "valley" is probably a preferentially etched subgrain boundary. Pits on the (001) surfaces are thermal in origin.

Figure 24 is a 2,000 magnification of the center of Fig. 23. Again the vicinal surface structure is obvious. Note that the "plateau" surface appears to be similar to the surface shown in Fig. 19 of the first sample.

E. Surface Composition Analysis

The samples were also analyzed using an electron microprobe, which provides the composition of any point on the sample surface. The unreacted sample, the reference, is found to have a uniform composition across the surface of Ga:As=1.00:1.00.

Sample #2, on the other hand, does not have a uniform composition across its surface. Refering to Fig. 23, a photograph of the relevant surface, the (001) flats are found to have a composition of Ga:As=1.06:1.00, which is

slightly enriched in gallium compared to the reference. The valley in Fig. 23, an etched subgrain boundary, has a composition of Ga:As=0.05:1.00, indicating a severe depletion of gallium. Since the (001) flats of sample #2 are similar in composition to the reference, it was judged unnecessary to examine sample #1 under the microprobe, because the composition probably lies somewhere between the flats of sample #2 and the reference.

It should be noted that the stoichiometric notation of Ga:As is merely a ratio of the mole fractions of each element on the surface and does not reflect the true chemical stoichiometry of the surface layer.

F. Equipment Observations

During the runs a grayish material deposited on the cooler sections of the reactor tube. On certain areas of the top endcap the deposit was absent where the HCl had not yet entered the tube, possibly indicating that HCl had to be present for its deposition. This seems unlikely, though, since the deposition also occurred before the HCl was bled in and during the free evaporation of GaAs. It would appear that the large inlet tube "shadowed" the inside surface at one point from the free gallium and arsenic present at such low pressure, and hence the deposit is probably gallium and arsenic.

After the runs the sample holder was examined and there was no deposit on the holder itself. Towards the top of the tube there was some deposit on the suspension fiber, which might affect the accuracy of the results. When the weight of the sample was compared to the weight as measured by the microbalance before and after reaction, the error was about 0.3% of the sample weight. This error is probably partially due to the fiber deposition, but is well within the experimental error of the entire study and hence can be ignored.

G. Errors of the Results

Estimation of errors in this type of study is difficult, for there are many individual measurements that contribute to the determination of any one quantity. The weakest link in this computation chain is the pressure measurements, which were done by taking differences in readings and are not absolute values. The next least reliable measurement is the temperature determinations, since thermocouples are not accurate sensors of rarified gas temperatures.

The activation energies, orders of reaction, and rate constants are probably not accurate to better than 10%.

One possible source of error would be the back reflection from the tube walls of GaCl, which might constitute a significant product partial pressure at the sample surface.

If a Knudsen regime is assumed, and that the deposition of material on the walls of the tube constitutes a GaCl concentration of zero, then a simple calculation can yield the partial pressure of GaCl at the sample surface; a typical computation is given in Appendix C. The partial pressure of GaCl at the surface of the sample is about 10^{-26} - 10^{-29} atm., depending on whether a Knudsen diffusion coefficient or a binary diffusion coefficient is used. These values are at most 10^{-15} of the equilibrium values for GaAs,[9] therefore the back-impingement is negligible.

V. DISCUSSION

This section will be concerned with interpreting the data presented in the results section, and follows the same format.

A. Free Evaporation of GaAs

It appears unlikely that there is only one single mechanism or single rate determining step for all the conditions studied, but an attempt will be made to propose a probable sequence of steps which will explain the observations.

In Fig. 9 it is noted that there can be two values (data points) for a single value of 1/T. Between data points the sample had been at a particular temperature T for several hours, in addition to undergoing reaction with HCl. In particular, points 1 and 22 reflect a surface which had been chemically polished, loaded into the reactor and heated; quite possibly the surface structure still had some kind of damage from the etch step and/or the surface structure had not yet equilibrated to the high temperature. The residual damage would mean the surface was roughened, allowing for more evaporation surfaces and hence higher evaporation rates, as is seen for points 1 and 22 in Fig. 9.

For the TLK model, the pressure-independent ledge spacing decreases with increasing temperature.[18] If the evaporation rate is proportional to the ledge density, then r_{THERM} should increase with increasing T, as is observed in Fig. 9 for high T. But it will require a certain relaxation time for the ledge spacing to equilibrate with a new temperature. If the sample is raised in temperature then there should be a temporary "shortage" of ledge sites at the new, higher temperature, and the evaporation rate will fall short of the equilibrated rate. This lag is observed in Fig. 9 for point 59 and not for points 1, 22, or 42. If the sample is lowered in temperature there should be an "excess" of ledge sites and the observed evaporation rate will be greater than the surface equilibrated rate. This behavior is exhibited by point 8 and not be point 15. It seems that any attempt to explain the deviations in Fig. 9 by equilibrated surface structure alone is inadequate, especially if a liquid gallium film forms on the surface.

Points 22 and 42 in Fig. 9 were obtained under a partial pressure of H_2 of 12 μmHg and fall exactly on the rate curve, as do points 41 and 53. Since p_{H_2} = 51 μmHg for point 53, it appears that the H_2 had little effect on the thermal evaporation rate, supporting that assumption which was made in the theory section. Points 22, 27 and 28 are not considered

valid since a later plot (Fig. 12) shows that points 23, 24, 25, and 26 are inconsistent; some sort of impurity is suspected.

The deviations of points 22-28 from the reasonable values given by the line drawn in Fig. 9 can be explained by a contamination of the surface of the sample. Points 1 and 22 were taken from a freshly-loaded GaAs sample whose surface was unreacted by HCl at the time. As time proceeds the deviations become less until for points 7 and 29 in Fig. 9 they are seen to be negligible. This suggests that there was some contaminant on the surface, either solid or vapor, which was removed by heat and/or HCl. Note that the only two points to follow the equilibrated surface theory described previously are points 8 and 59, points which were taken after the contaminant was removed. It is common for gases and liquids to catalyze surface evaporation. Specifically, Lou[9] found that a liquid gallium film placed on a (111) GaAs crystal increased the free evaporation rate by a factor of about two. Therefore a surface contaminant might be expected to increase the evaporation rate by catalysis, as is shown in Fig. 9.

Since the Arrhenius plot in Fig. 9 curves, the apparent activation energy for the evaporation process is not constant. In the same figure an extrapolation of Lou's[9]

study on (111) GaAs evaporation is shown, the slope of which gives an activation energy of 90 kcal/mole. It appears that the high T asymptote of the present study in Fig. 9 would approach Lou's slope if the temperature range studied had been extended. The activation energy value of 72 kcal/mole obtained here is thus expected to be low, and should approach Lou's value of 90 kcal/mole. The evaporation rate of (001) GaAs is expected to be higher than for (111) GaAs, because a study of Sangster's[10] work shows that the (001) surface is more uniformly accessable from a bonding standpoint than the (111) surface.

The change in activation energies shown in Fig. 9 from 72 to 14 kcal/mole as T decreases is probably not a change in the mechanism, but rather a change in the rate determining step. Lou proposed the rate limiting step is the formation of the divacancy $[V_{Ga}V_{As}]$ at temperatures above 800°C. Considering the downward trend of the activation energy as the temperature decreases, it is probable that a parallel step becomes dominant at the lower temperature.

Goettler[6] used a known boundary layer to derive the surface kinetics for (100) GaAs epitaxy. The growth rate was expressed as a function of the chemical affinity of the substrate surface. Figure 18 is a plot of Goettler's rate

constant k versus 1/T. His data exhibits the same apparent change of rate determining step as the data from this study, and the change occurs at approximately the same temperature range. The asymptotes of Fig. 18 yield activation energies for the deposition of (100) GaAs of 89.3 kcal/mole for the high T range and 11.0 kcal/mole for the low T region. These values compare favorably to the 72 and 14 kcal/mole obtain in the present study, especially since the energies obtained here will approach Goettler's values as pointed out in the results section.

The stoichiometry for Goettler's reaction is the same as that for the GaAs evaporation. To say that the actual mechanisms are the same for both deposition and evaporation is not really justified, however. It is possible that the similarity in the activation energies is coincidence.

B. Pure HCl Reaction with GaAs

Figure 10 gives the order of reaction with respect to HCl, n, a value of from 0.96 to 1.45. The 735.5°C line, which yields the 1.45 value, appears to be somewhat time dependent because the slope approaches that of the other temperatures as time proceeds. The n value of 1.45 is then too high and should be disregarded. A reasonable value of n is about unity for pure HCl.

The time dependency of the 735.5°C line in Fig. 10 is more obviously duplicated in Fig. 11 for 736°C. The time

dependency, described previously in the results section, is best explained by the contaminant hypothesis. The impurity catalyzed the surface reaction and led to a false high order of reaction.

Since n=1, one molecule of HCl is required per atomic (molecular) reaction. The most probable site for HCl attack is at the ledges on the surface of the GaAs. The sequence for atomic adsorption on the surface as pressure increases is ledge, then terrace, and finally the entire surface becomes saturated. The surface free energy is also decreased by adsorbing species,[23] hence the evaporation rate (production of adatoms or vapor) is increased. It is then proposed that the HCl adsorbs on the ledge sites, forms a complex with Ga, and either vaporizes directly or becomes adsorbed on the terrace, surface diffuses, and then vaporizes. The mechanism is illustrated in Table 4b.

The apparent activation energy of zero can be explained by the adsorption of the impinging molecules into a deep potential well as they approach the surface. If thermal accommodation is good, then their adsorption into the deep well will give a zero activation energy; this is not uncommon for vacuum reactions at elevated temperatures.

C. HCl Reaction with GaAs with H_2 Present

Figure 12 shows that the curve drawn through points 23-26 is quite different than the other curves in the same figure, and in Fig. 13. The data obtained from sample #2 began with point 22, and if the surface were contaminated there should be a decreasing deviation with time. This is observed, with points 23 and 24 further from the expected rate than points 25 and 26. Again, the surface impurity theory is supported.

Comparison of Figs. 12 and 13 with Fig. 10 indicates that the combined rate r_c is lower than the pure HCl rate r_{HCl} for the same p_{HCl}. For high partial pressures of HCl, about 80 μmHg, the rates are depressed by about 10%, while at HCl pressures of about 17 μmHg the rates are decreased by about 20% by the addition of hydrogen. It is obvious that the hydrogen is somehow interferring with the HCl-GaAs reaction. Examination of Figs. 14 and 15 show the rate is maximized as a function of p_{HCl} in the presence of hydrogen; the same shape curve is given in Fig. 4 for the

D. Proposed Mechanism for the HCl-GaAs Reaction

Based on the experimental evidence it is possible at this point to propose a reaction mechanism for the HCl-H_2-GaAs system. The rate limiting step must be first order with respect to HCl, and have an activation energy somewhere near zero. The slowest step must be further slowed by the addition of hydrogen.

The proposed mechanism is presented in Table 4b. The HCl vapor adsorbs intact on the ledge position; this adsorption step is rate determining. The adsorbed HCl is in equilibrium with its dissociated components at the ledge position. Gallium on the ledge and Cl combine to form GaCl at the ledge position. The direct vaporization from ledge sites is generally not favored (see theory section); the ledge GaCl will move to the terrace and then desorb.

Note that the addition of H_2 (which dissociates on the surface) will shift the equilibrium concentration of Cl atoms on on the surface. The adsorption of HCl and the desorption of H are then at equilibrium as described in Table 4c; the rate determining step now becomes the combination of the adsorbed Cl and Ga atoms.

For the reaction with HCl only the rate is proportional to the partial pressure of HCl, since it is adsorption limited. Specifically, the observed rate may be expressed as some reaction probability or fraction P_r of the impingement rate:

$$r_{ads} = \frac{P_r r_{HCl}}{(2\pi mkT)^{1/2}} \qquad (24)$$

Typically, the impingement rate is 10^{18} molecules/cm^{2}sec, and the observed rate is 10^{15}. The resulting reaction

probability of 0.001 is not unreasonable, since only the ledge sites are reactive which constitute some small (< 0.1) fraction of the total surface area. Madix and Schwartz[21] obtained reaction probabilities which decrease rapidly with decreasing temperature for Cl_2 reaction with Si and Ge.

When H_2 is added the adsorption equilibria are shifted and the combination of $Ga_{(L)}$ and $Cl_{(L)}$ controls the overall rate. For this mechanism, given in Table 4c, the rate is given by:

$$r = \frac{k\ K_a p_{HCl}/(K_b^{1/2} p_{H_2}^{1/2})}{(1 + K_b^{1/2} p_{H_2}^{1/2} + K_a p_{HCl}/K_d^{1/2} p_{H_2}^{1/2})^2} \qquad (25)$$

This expression can be maximized with respect to p_{HCl}, as sketched in Fig. 4. The maximum rate is obtained for the following value of p_{HCl}:

$$(p_{HCl})_{MAX} = (K_b^{1/2} p_{H_2}^{1/2} + 1)(K_b^{1/2} p_{H_2}^{1/2})/K_a \qquad (26)$$

The derivation of these equations is given in Appendix D.

It normally would be possible to evaluate the unknown adsorption equilibrium constants K_a and K_d, and the total covered fraction θ_T of the surface from the type of data obtained in this study. Unfortunately, this interpolation is prevented by the imprecision and uncertainty in the curves shown in Figs. 15-18. However, the rate equation does predict the maximum rates exhibited by the data.

E. Role of As in the GaAs-HCl-H_2 System

In the discussion thus far the fate of the arsenic atoms has been ignored for the various reactions. It is likely that the the As atoms do not influence the mechanisms previously described, because of the alternating terraces of Ga and As atoms. The mechanisms outlined occur on the Ga terraces.

During etching HCl and H_2 are certain to adsorb on the As terraces and ledges as well, but the As combines into the dimer and tetramer without reacting with either gas species due to the thermodynamic unfavorability. The polymerization of the As atoms is included in Tables 4a and 4b, as originally suggested by Lou.[9]

F. Reaction Rate Equation

For pure HCl reacting with GaAs the rate may be approximated by:

$$r_{HCl} = (9.4\ 10^{-6})(p_{HCl})^{1.11} \qquad (27)$$

where r_{HCl} is in units of [mg-cm^{-2}-sec^{-1}] and p_{HCl} is in [μmHg]. This equation is derived from Fig. 10, for temperatures 662.64°, 704.79°, and 687.43°C.

The reaction rate for HCl with GaAs in the presence of H_2 cannot be written in the above form since the rate is maximized.

Equation 27 is valid for total pressure equalling p_{HCl} and not exceeding 135 μmHg, and for temperatures 660°C < T < 705°C, although the temperature limits can be extended somewhat.

G. Surface Morphology of GaAs

In general, the etched surface structure of GaAs was a consequence of the more reactive planes reacting fastest, leaving the slower etching planes remaining. From the SEM photomicrographs the slowest etching planes appeared to be the (001) and (111) planes. The equilibrium crystal structure was not exhibited by the samples since the reaction was far from equilibrium.

The electron microprobe analysis of sample #2 suggests that GaAs reaction with HCl and further evaporation result in an enrichment of gallium on the surface, relative to the reference sample. It would appear that the arsenic evaporates faster than the gallium until some steady-state surface composition of Ga:As = 1.06:1.00 is obtained. The ratio also suggests that a thin layer of liquid gallium may form on the surface. The thickness of the layer is most likely less than a micron, considering the beam voltage was 15 kv. But even a few monolayers is sufficient to invalidate the application of the TLK model. However, comparison of Figs. 9 and 10 shows that r_{HCl} is always greater that r_{THERM}, and examination of Figs. 12-15 show this to be true for r_c as well. It can be stated that the liquid Ga layer does not form while HCl is present in the quantities used here, and that the TLK model does apply when GaAs is etched with HCl (and H_2 + HCl). It

seems that the layer forms only during the thermal evaporation of GaAs, and the corresponding mechanism proposed by Lou[9] is shown in Table 4a.

The valleys of sample #2 were extremely depleted of Ga, as seen in Fig. 22. The reactants and products then have to diffuse through a layer of arsenic. It is difficult to estimate what percentage of the surface area consists of these valleys, but is probably about 10-20%, and imparts a comparable error in the observed kinetics, since an As layer is not assumed.

The SEM photograph of Fig. 19 shows white material surrounding the etch pits. The dislocation density would be too high to account for such pitting. It is suggested that the white material is the contaminant which has evidenced itself throughout the discussion. It is thought that the impurity was picked up by the chemical etching procedure, probably a metallic compound which reacted with the HCl to form a stable chloride, the white material on the surface. Wherever the metallic compound was on the surface an etch pit formed, which accounts for the high etch pit density. It might be thought that the contaminant was oxygen, but that fails to explain the erroneous initial data points, and the point by point spotting of the surface in Fig. 19. In addition, it is not known where the oxygen could come from in the system. The observations indicate some metallic compound as the impurity.

VI. CONCLUSION

The thermal evaporation and reaction of (001) GaAs with HCl and H_2 is investigated using differential gravimetry. Two kinetic regimes is found for the free evaporation of (001) GaAs, with activation energies of 72 kcal/mole and 14 kcal/mole for the high and low temperature regions respectively. Comparable activation energies obtained by others for the deposition of (100) GaAs and the free evaporation of (111) GaAs confirm the validity of the present data.

The reaction between (001) GaAs and HCl is found to have an order of reaction with respect to HCl of about unity, and can be approximated by:

$$r_{HCl} = (9.4\times10^{-6})(p_{HCl})^{1.11}$$

valid for $660 < T < 705°C$ and $0 < p_{HCl} < 135$ μmHg. This relation is actually for the surface reaction in pure HCl. The mechanism is believed to be the adsorption of HCl on ledge sites which forms a complex with Ga and desorbs.

The presence of H_2 in the vapor phase with HCl complicates the kinetics of the reaction with GaAs. The rate is found to depend on both hydrogen and hydrogen chloride partial pressure. The hydrogen has a zero order

of reaction at low pressures, and retards the HCl reaction at higher pressures, depending on temperature. The H_2 uniformly decreases the HCl rate by 10-20% at low pressures and the rate is independent of H_2 over a wide range of p_{H_2}. Zero activation energies are obtained for HCl reaction alone and for the same reaction with H_2 present in the vapor phase.

The surface structure is found to be composed of the slowest etching planes of (001) and (111) surfaces. Thermal etching is evident on the vicinal surfaces. The surface is enriched in Ga slightly by the simultaneous evaporation and HCl etching, although the subgrain boundaries are preferentially etched by the HCl. The result is an As layer over the boundaries, which may amount to 10-20% of the total surface area.

It can be concluded that the GaAs-HCl-H_2 system is extremely difficult to model in a quantitative way. Even if a model exists for the evaporation of a dissociating solid, the complications of As and Ga rich layers on the surface, HCl adsorption, and H_2 interference will further restrict the analysis. Essentially, the difficulties of modelling the present system are:

1. The GaAs dissociates at high temperatures.
2. The thermal evaporation of GaAs has two kinetic regions.
3. At high temperatures the formation of a liquid Ga layer is possible.
4. The adsorption equilibria of HCl and H_2 on GaAs is unknown.
5. The formation of an As layer on subgrain boundaries complicates the surface reaction.

The reacting surface of GaAs is extremely complex, and will pose a difficult modelling problem for some time to come.

It is recommended that further work be done on the system utilizing LEED and molecular beam apparatus.

ACKNOWLEDGEMENTS

I would like to offer my sincerest appreciation to the following, for without their dedication and effort my work would not have been possible: Carl Baugh and Slim Bohac of the machine shop; Dane Anderberg and Paul Hendrickson of the glass shop; Brian Pope and George Georgakopoulos of IMRD; Nancy Monroe, for the drafting; and Alice Ramirez, Shirley Ashley and Jean Wolslegel for the preparation of the final manuscript.

Leroy McIntosh, Jr. and Lucius Winn deserve special commendation for their encouragement during the many long nights made necessary by this work. I am also most grateful for the friendship offered by my research compatriots Ray Pong, Terry Ring, Gary Arbach and Pravin Mundkur; our mutual discussions helped set the proper attitude for my endeavors. Patience and understanding were constantly offered by Tonia, truest of all friends.

In the academic ivory towers my thanks go to Professor Merril for his many useful comments; to Professor Morris for clarifying my goals in this dissertation, and of course I must thank Professor Donaghey for his constant influence throughout my program.

This work was supported by the U. S. Atomic Energy Commission.

APPENDIX A.
MEAN FREE PATH OF HCl

The mean free path may be expressed as:[26]

$$\lambda = \frac{1}{\sqrt{2}\pi d^2 n_c}$$

where λ = mean free path

d = diameter of spherical molecules

n_c = concentration, molecules/unit volume

n_c can be written as:

$$n_c = \frac{(6.023\times10^{23})p}{RT}$$

For HCl, $d_{HCl} = 3.305\times10^{-8}$ cm (from Reference 27), and at 370°C,

$$n_c = \frac{(7.34\times10^{21})p}{(1.003\times10^{3})}$$

where p is in atmospheres. For 100 μmHg pressure, λ_{HCl} is 370°C. For 8 μmHg pressure, λ_{HCl} is 2.68 cm for 730°C.

APPENDIX B
DATA POINTS

Point No.	Run No.	Average Temp. (°C)	Gases Present	p_{TOTAL} (μm Hg)	p_{HCl} (μm Hg)	p_{H_2} (μm Hg)	$r_{TOT} \times 10^4$ (mg-cm²-sec)	Comments
1	1	736.76	NONE	28	0	0	5.77	HEATED FROM ROOM TEMPERATURE
2	1	"	HCl	103	92	0	7.69	
3	1	"	HCl	59	48	0	5.07	
4	1	"	HCl	35	24	0	4.77	
5	1	"	HCl	90	79	0	8.62	
6	1	"	HCl	175	164	0	18.2	
7	1	"	NONE	11	0	0	4.62	TIME AT 736.76°C = 4 HOURS
8	1	704.79	NONE	6	0	0	1.87	COOLED FROM 736.76°C
9	1	"	HCl	106	96	0	12.5	
10	1	"	HCl	53	43	0	6.59	
11	1	"	HCl	22	12	0	2.96	
12	1	"	HCl	95	85	0	11.0	

APPENDIX B
DATA POINTS

Point No.	Run No.	Average Temp. (°C)	Gases Present	p_{TOTAL} (μm Hg)	p_{HCl} (μm Hg)	p_{H_2} (μm Hg)	$r_{TOT} \times 10^4$ (mg-cm^2-sec)	Comments
13	1	704.79	HCl	155	145	0	8.23	
14	1	"	NONE	10	0	0	1.49	TIME AT 704.79°C = 3½ HOURS
15	1	662.84	NONE	2	0	0	0.708	COOLED FROM 704.79°C
16	1	"	HCl	40	38	0	5.93	
17	1	"	HCl	20	18	0	2.85	
18	1	"	HCl	72	70	0	12.3	
19	1	"	HCl	103	101	0	17.5	
20	1	"	HCl	135	133	0	25.3	
21	1	"	NONE	2	0	0	0.710	TIME AT 662.84°C = 3 HOURS
22	2	629.99	H_2	20	0	12	1.22	HEATED FROM ROOM TEMPERATURE
23	2	"	$HCl+H_2$	75	55	12	3.53	
24	2	"	$HCl+H_2$	243	53	182	9.48	

APPENDIX B
DATA POINTS

Point No.	Run No.	Average Temp. (°C)	Gases Present	p_{TOTAL} (μm Hg)	p_{HCl} (μm Hg)	p_{H_2} (μm Hg)	$r_{TOT} \times 10^4$ (mg-cm^2-sec)	Comments
25	2	629.99	$HCl+H_2$	200	51	141	7.37	
26	2	"	$HCl+H_2$	100	49	43	4.54	
27	2	"	H_2	51	0	43	1.44	
28	2	"	H_2	20	0	12	0.622	
29	2	"	$HCl+H_2$	38	16	12	1.87	
30	2	"	$HCl+H_2$	40	16	16	2.18	
31	2	"	$HCl+H_2$	38	17	13	2.21	
32	2	"	$HCl+H_2$	70	17	45	2.24	
33	2	"	$HCl+H_2$	90	17	65	1.92	
34	2	"	$HCl+H_2$	119	18	93	1.85	
35	2	"	$HCl+H_2$	38	18	12	2.28	
36	2	"	$HCl+H_2$	60	40	12	4.65	

APPENDIX B
DATA POINTS

Point No.	Run No.	Average Temp. (°C)	Gases Present	p_{TOTAL} (μm Hg)	p_{HCl} (μm Hg)	p_{H_2} (μm Hg)	$r_{TOT} \times 10^4$ (mg-cm^2-sec)	Comments
37	2	630.50	$HCl+H_2$	145	40	97	4.07	
38	2	"	$HCl+H_2$	128	40	80	4.38	
39	2	"	$HCl+H_2$	100	39	52	4.87	
40	2	"	$HCl+H_2$	59	39	12	4.89	
41	2	"	H_2	20	0	12	0.487	TIME AT 630°C = 12 HOURS
42	2	685.56	H_2	20	0	12	1.03	HEATED FROM 630°C
43	2	"	$HCl+H_2$	105	85	12	1.04	
44	2	"	$HCl+H_2$	130	85	37	10.3	
45	2	"	$HCl+H_2$	156	80	68	10.3	
46	2	"	$HCl+H_2$	107	75	24	12.0	
47	2	686.86	$HCl+H_2$	120	71	41	12.4	
48	2	"	$HCl+H_2$	82	33	41	5.45	

APPENDIX B
DATA POINTS

Point No.	Run No.	Average Temp. (°C)	Gases Present	p_{TOTAL} (μm Hg)	p_{HCl} (μm Hg)	p_{H_2} (μm Hg)	$r_{TOT} \times 10^4$ (mg-cm²-sec)	Comments
49	2	686.86	$HCl+H_2$	100	33	59	5.29	
50	2	"	$HCl+H_2$	117	33	76	5.02	
51	2	"	$HCl+H_2$	129	33	88	4.85	
52	2	"	$HCl+H_2$	92	33	51	5.32	
53	2	687.43	H_2	59	0	51	0.865	
54	2	"	NONE	8	0	0	1.13	
55	2	"	HCl	55	47	0	8.03	
56	2	"	HCl	38	30	0	4.96	
57	2	"	HCl	125	117	0	19.5	
58	2	"	NONE	8	0	0	1.13	TIME AT 687°C = 9½ HOURS
59	2	735.50	NONE	10	0	0	3.65	HEATED FROM 687°C
60	2	"	HCl	62	52	0	9.72	

APPENDIX B
DATA POINTS

Point No.	Run No.	Average Temp. (°C)	Gases Present	p_{TOTAL} (μm Hg)	p_{HCl} (μm Hg)	p_{H_2} (μm Hg)	$r_{TOT} \times 10^4$ (mg-cm²-sec)	Comments
61	2	735.50	HCl	111	101	0	21.0	
62	2	"	HCl	187	177	0	38.1	
63	2	"	NONE	10	0	0	4.17	TIME AT 735.50°C = 2 HOURS

APPENDIX B

TABLE I

SAMPLE SPECIFICATIONS

Sample (Run) No.	Initial Weight (gm)	Final Weight (gm)	Surface Area Both Sides (cm^2) Initial	Surface Area Both Sides (cm^2) Final	Average Surface Area (cm^2)	Final Appearance
1	0.5417	0.3826	5.8345	5.6636	5.7491	Surface slightly rougher than before reaction; see Figure 20.
2	0.5326	0.3915	5.4569	5.4569	5.4569	Surface extremely rough; see Figures 21-25.

APPENDIX C

Back Reflection Calculation

Assume that the concentration of GaCl is zero at the point in the tube where the gray material begins to condense on the tube walls, and call the distance between this point and the sample L(=33 cm. as measured). The flux of material down the tube is given by

$$\frac{\text{rate}}{A} = -D\,\frac{dC}{dL} = -D\,\frac{(C_s - 0)}{L}$$

at steady state conditions. For a first approximation assume the diffusion coefficient D is equal to a Knudsen diffusion coefficient, D_{Knud}, which can be expressed as the following for a tube of radius r:[28]

$$D_{Knud} = \frac{-2r}{3}\left(\frac{8\ RT}{\pi M}\right)^{1/2}$$

For a tube of radius 2.5 cm, $D_{Knud} = -2.36\times10^{3}\ T^{1/2}$, and the cross sectional area is 19.62 cm^2. For p_{HCl} of 15 μmHg and T=1000°K, the observed rate is 1.75×10^{-4} mg/cm^2sec of GaAs reacted. C_s is then 7.2×10^{-12} $moles/cm^3$, and the resulting partial pressure of GaCl at the sample surface is 8.6×10^{-30} atmospheres.

If a binary diffusion coefficient is assumed, using Lennard-Jones for its computation, the partial pressure of GaCl is about 1.4×10^{-26} atmospheres.

APPENDIX D

HCl/H_2 Rate Equation

With H_2 in the vapor phase the mechanism shown in Table 4c can be written as

$$HCl_{(v)} \underset{k_{-1}}{\overset{k_1}{\rightleftharpoons}} H_{(L)} + Cl_{(L)} \tag{A}$$

$$Ga_{(L)} + Cl_{(L)} \xrightarrow{k_r} GaCl_{(L)} \tag{B}$$

$$H_{2(v)} \underset{k_{-2}}{\overset{k_2}{\rightleftharpoons}} 2H_{(L)} \tag{C}$$

The rate of reaction may be expressed as

$$r = k\ \theta_{Cl}(1-\theta_{Cl}-\theta_H) \tag{D}$$

The sum of θ_{Cl} and θ_H is θ_T, the fraction of the ledge sites covered.

Steps (A) and (C) are equilibrium reactions, so

$$k_1\ p_{HCl}(1-\theta_T)^2 = k_{-1}\ \theta_H\ \theta_{Cl} \tag{E}$$

and

$$k_2\ p_{H_2}(1-\theta_T)^2 = k_{-2}\ \theta_H{}^2 \tag{F}$$

Rearranging,

$$\frac{\theta_H \ \theta_{Cl}}{(1-\theta_T)^2} = K_a \ p_{HCl} \qquad \text{(G)}$$

and

$$\frac{\theta_H}{(1-\theta_T)} = K_b^{1/2} \ p_{H_2}^{1/2} \qquad \text{(H)}$$

where

$$K_a = \frac{k_1}{k\text{-}1} \quad \text{and} \quad K_b = \frac{k_2}{k\text{-}2} \ .$$

Eliminating θ_H and solving for $(1-\theta_T)$ from (G) and (H),

$$(1-\theta_T) = \theta_{Cl} \ \frac{K_b^{1/2} \ p_{H_2}^{1/2}}{K_a \ p_{HCl}} \qquad \text{(I)}$$

Insertion of (I) in (D) gives

$$r = k\theta_{Cl}^2 \ \frac{K_b^{1/2} \ p_{H_2}^{1/2}}{K_a \ p_{HCl}} \qquad \text{(J)}$$

From (H),

$$\theta_H = \frac{K_b^{1/2} \ p_{H_2}^{1/2} \ (1-\theta_{Cl})}{1 + K_b^{1/2} \ p_{H_2}^{1/2}} \qquad \text{(K)}$$

Subsituting (K) into (I) and rearranging,

$$\theta_{Cl} = \frac{K_a\ p_{HCl}/K_b^{1/2}\ p_{H_2}^{1/2}}{1 + K_b^{1/2}\ p_{H_2}^{1/2} + \dfrac{K_a\ p_{HCl}}{K_b^{1/2}\ p_{H_2}^{1/2}}} \qquad \text{(L)}$$

Substitution of (L) into (J) yields

$$r = \frac{k\ \dfrac{K_a\ p_{HCl}}{K_b^{1/2}\ p_{H_2}^{1/2}}}{\left(1 + K_b^{1/2}\ p_{H_2}^{1/2} + \dfrac{K_a\ p_{HCl}}{K_b^{1/2}\ p_{H_2}^{1/2}}\right)^2} \qquad \text{(M)}$$

Taking the derivative with respect to p_{HCl}, setting it equal to zero, and solving for p_{HCl} gives

$$(p_{HCl})_{MAX} = \frac{(K_b^{1/2}\ p_{H_2}^{1/2} + 1)(K_b^{1/2}\ p_{H_2}^{1/2})}{K_a} \qquad \text{(N)}$$

where $(p_{HCl})_{MAX}$ is the HCl partial pressure corresponding to the maximum rate, as shown in Fig. 4. Note that as $p_{H_2} \to 0$, $(p_{HCl})_{MAX} \to 0$, which is not consistent with the data; however, (M) does reflect the observed maximum rates.

REFERENCES

1. T. Acharya, D. Olander, Carbon 11(1), (1963).
2. D. Olander, I&EC Fund. 6, 188 (1967).
3. E. Sparrow, J. Gregg, ASME Transactions, J. of Heat Transfer, Nov. 1960.
4. D. Rosner, H. Allendorf, AIAA J. 6, 650 (1968).
5. G. Blyholder, H. Eyring, J. Phys. Chem. 61, 682 (1957).
6. L. Goettler, "Diffusion and Surface Kinetics in the Expitaxial Vapor Deposition of Gallium Arsenide," 1970, Monsanto Co., St. Louis, Mo.
7. D. Shaw, J. Elect. Soc. 117, 683 (1970).
8. T. O. Sedgwick, J. Elect. Soc. 111, 1381 (1964).
9. C. Lou, Lawrence Berkeley Laboratory Report No. 19685, (1970), Berkeley, California.
10. R. C. Sangster, Compound Semiconductors in Preparation of III-V Compounds, R. K. Willardson and H. L. Goering, eds. (Reinhold Publishers Corp., New York, 1962), Vol. 1, Chap. 28.
11. D. J. Kirwan, J. Elect. Soc. Solid State Science 117, 1572 (1970).
12. W. W. Mullins, Metal Surfaces (ASM, Ohio, 1963).
13. K. A. Jackson, Progress in Solid State Chemistry, H. Reiss, ed. (Pergamon Press, Oxford, 1967), Vol. 4.
14. A. J. W. Moore, Metal Surfaces (ASM, Ohio, 1963).
15. V. Ban, J. Crystal Growth 17, (1972).

16. G. A. Somorjai and N. R. Stemple, J. Appl. Phys. 35, 3398 (1953).

17. G. A. Somorjai, J. E. Lester, Progress in Solid State Chemistry, H. Reiss, ed. (Pergamon Press, Oxford, 1967), Vol. 4.

18. J. P. Hirth and G. M. Pound, J. Chem. Phys. 26, 1216 (1957).

19. N. A. Gjostein, Metal Surfaces (ASM, Ohio, 1963).

20. J. R. Arthur, Surface Science 38, 1973.

21. R. J. Madix and J. A. Schwarz, Surface Science 24, (1971).

22. R. J. Madix, A. A. Susu, J. of Vacuum Science and Technology, 9(2), (1972).

23. R. J. Madix, R. Parks, A. A. Susu and J. A. Schwarz, Surface Science 24, (1971).

24. P. G. Shewman and W. M. Robertson, Metals Surfaces (ASM, Ohio, 1973).

25. K. J. Laidler, Chemical Kinetics (McGraw-Hill, New York, 1965), 2nd edition.

26. R. B. Bird, W. E. Stewart, E. N. Lightfoot, Transport Phenomena (J. Wiley & Sons, New York, 1960).

27. J. O. Hirshfelder, C. F. Curtiss and R. B. Bird, Molecular Theory of Gases and Liquids (J. Wiley, New York, 1954).

28. T. K. Sherwood, R. L. Pigford and C. R. Wilke, Mass Transfer (to be published by McGraw-Hill, N. Y.).

TABLE 1

ΔF FOR ATOMIC MOVEMENT[18]

Position Change ΔF Activation	ΔF_0 Kink To Ledge	ΔF_1 Ledge To Adsorbed	ΔF_3 Adsorbed To Vapor	ΔF_5 Ledge To Vapor	ΔF_D Surface Diffusion	To Form Kink in Ledge	Kink To Vapor	Vapor From in Surface
fcc (111)	ϕ	2ϕ	$3\phi+3\phi'$	$5\phi+3\phi'$	$< \phi$	$\phi/2$	$6\phi+3\phi'$	$9\phi+3\phi'$
fcc (001)	ϕ'	$2\phi+\phi'$	$4\phi+\phi'$	$6\phi+2\phi'$	$< \phi$	$\phi'/2$	$6\phi+3\phi'$	$8\phi+5\phi'$
Simple cubic (100)	ϕ	$\phi+2\phi'$	$\phi+4\phi'$	$2\phi+6\phi'$	$< \phi$	$\phi/2$	$3\phi+6\phi'$	$5\phi+8\phi'$
Simple cubic (110)	ϕ'	ϕ	$2\phi+5\phi'$	$3\phi+5\phi'$	$< \phi$	$\phi/2$	$3\phi+6\phi'$	$4\phi+7\phi'$

TABLE 2

k_i For GaAs

$T=1000^{o}K$

i	k_i (sec^{-1})
1	10
3	10^{-11}
5	10^{-23}

TABLE 3

PROBABLE SURFACE MECHANISMS

LEDGE REACTIONS

1.a. $HCl_{(V)} \rightleftharpoons HCl_{(L)} \rightleftharpoons H_{(L)} + Cl_{(L)}$

b. $HCl_{(V)} \rightleftharpoons H_{(L)} + Cl_{(L)}$

c. $Ga_{(L)} + Cl_{(L)} \rightleftharpoons GaCl_{(L)}$

d. $HCl_{(L)} + Ga_{(L)} \rightleftharpoons GaCl_{(L)} + H_{(L)}$

e. $GaCl_{(L)} \longrightarrow GaCl_{(T)} \longrightarrow GaCl_{(V)}$

f. $GaCl_{(L)} \longrightarrow GaCl_{(V)}$

g. $2H_{(L)} \rightleftharpoons 2H_{(T)} \rightleftharpoons H_{2(T)} \rightleftharpoons H_{2(V)}$

h. $2H_{(L)} \rightleftharpoons H_{2(L)} \rightleftharpoons H_{2(V)}$

TERRACE REACTIONS

2.a. $HCl_{(V)} \rightleftharpoons HCl_{(T)} \rightleftharpoons H_{(T)} + Cl_{(T)}$

b. $HCl_{(V)} \rightleftharpoons H_{(T)} + Cl_{(T)}$

c. $Ga_{(T)} + Cl_{(T)} \rightleftharpoons GaCl_{(T)}$

d. $HCl_{(T)} + Ga_{(T)} \rightleftharpoons GaCl_{(T)} + H_{(T)}$

e. $GaCl_{(T)} \longrightarrow GaCl_{(V)}$

TABLE 3 (continued)

RIDEAL REACTION

5.a. $HCl_{(V)} + Ga_{(T)} \rightleftharpoons GaCl_{(T)} + H_{(V)}$

b. $GaCl_{(T)} \longrightarrow GaCl_{(V)}$

Nomenclature: (V) denotes vapor, (T) denotes terrace, (L) denotes ledge

TABLE 4

a. <u>(001) GaAs Vaporization Mechanism</u>

(from Lou[9])

1. $Ga_{Ga} \rightleftharpoons V_{Ga} + Ga_{(surface)}$

2. $Ga_{(surface)} \rightleftharpoons Ga_{(liquid)}$

3. $As_{As} \rightleftharpoons V_{As} + As_{(surface)}$

4. $V_{Ga} + V_{As} \rightarrow [V_{Ga}V_{As}]\bullet$

5. $[V_{Ga}V_{As}]_{(bulk)} \rightleftharpoons [V_{Ga}V_{As}]_{(surface)}$

6. $nV_{Ga}V_{As} \bullet 4As \rightleftharpoons As_{4(surface)}$

7. $As_{4(surface)} \rightarrow As_{4(V)}$

8. $n'V_{Ga}V_{As} \bullet 2As \rightleftharpoons As_{2(surface)}$

9. $As_{2(surface)} \rightarrow As_{2(V)}$

10. $Ga_{(liquid)} \rightarrow Ga_{(V)}$

Table 4

b. (001) GaAs Reaction with HCl

1. $HCl_{(v)} \rightarrow HCl_{(L)} \rightleftharpoons H_{(L)} + CL_{(L)}$
2. $Ga_{(L)} + Cl_{(L)} \rightleftharpoons GaCl_{(L)} \rightleftharpoons GaCl_{(T)}$
3. $GaCl_{(T)} \rightarrow GaCl_{(v)}$
4. $H_{2(v)} \rightleftharpoons 2H_{(L)}$
5. $H_{2(v)} \rightleftharpoons 2H_{(T)} \rightleftharpoons 2H_{(L)}$

TABLE 4

c. (001) GaAs Reaction with HCl/H_2

1. $HCl_{(V)} \rightleftharpoons HCl_{(L)} \rightleftharpoons H_{(L)} + Cl_{(L)}$

2. $Cl_{(L)} + Ga_{(L)} \longrightarrow GaCl_{(L)} \longrightarrow GaCl_{(T)}$

3. $GaCl_{(T)} \longrightarrow GaCl_{(V)}$

4. $H_{2(V)} \rightleftharpoons 2H_{(L)}$

5. $H_{2(V)} \rightleftharpoons 2H_{(T)}$

6. $H_{(T)} \rightleftharpoons H_{(L)}$

FIGURE CAPTIONS

Fig. 1. GaAs Unit Cell.

Fig. 2. Ideal Surface of (001) GaAs.

Fig. 3. Sample Orientation.

Fig. 4. Maximized Rate Behavior.

Fig. 5. TLK Model.

Fig. 6. Apparatus Schematic.

Fig. 7. Flow System.

Fig. 8. Typical Temperature Profile.

Fig. 9. r_{THERM} vs. 1/T.

Fig. 10. $-\ln r_{HCl}$ vs. $\ln p_{HCl}$ (various T).

Fig. 11. $-\ln r_{HCl}$ vs. $\ln p_{HCl}$ (T=736°C)

Fig. 12. $-\ln r_C$ vs. $\ln p_{H_2}$ (T=630°C)

Fig. 13. $-\ln r_C$ vs. $\ln p_{H_2}$ (T-686°C)

Fig. 14. $-\ln r_C$ vs. $\ln p_{HCl}$ (T-630°C)

Fig. 15. $-\ln r_C$ vs. $\ln p_{HCl}$ (T=686°C)

Fig. 16. r_C vs. p_{HCl} (T=630°C)

Fig. 17. r_C vs. p_{HCl} (T=686°C)

Fig. 18. k_s vs. 1/T

Fig. 19. Sample #1 (2,000X)

Fig. 20. Sample #2 (500X)

Fig. 21. Sample #2 (2,000X)

Fig. 22. Sample #2 (2,000X)

Fig. 23. Sample #2 (300X)

Fig. 24. Sample #2 (2,000X)

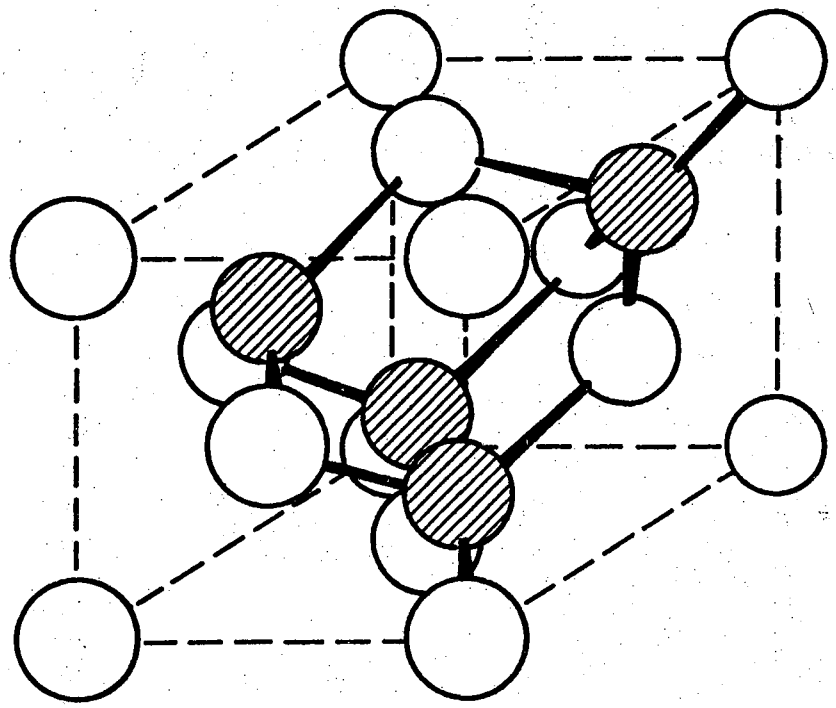

XBL 745-6223

Fig. 1.

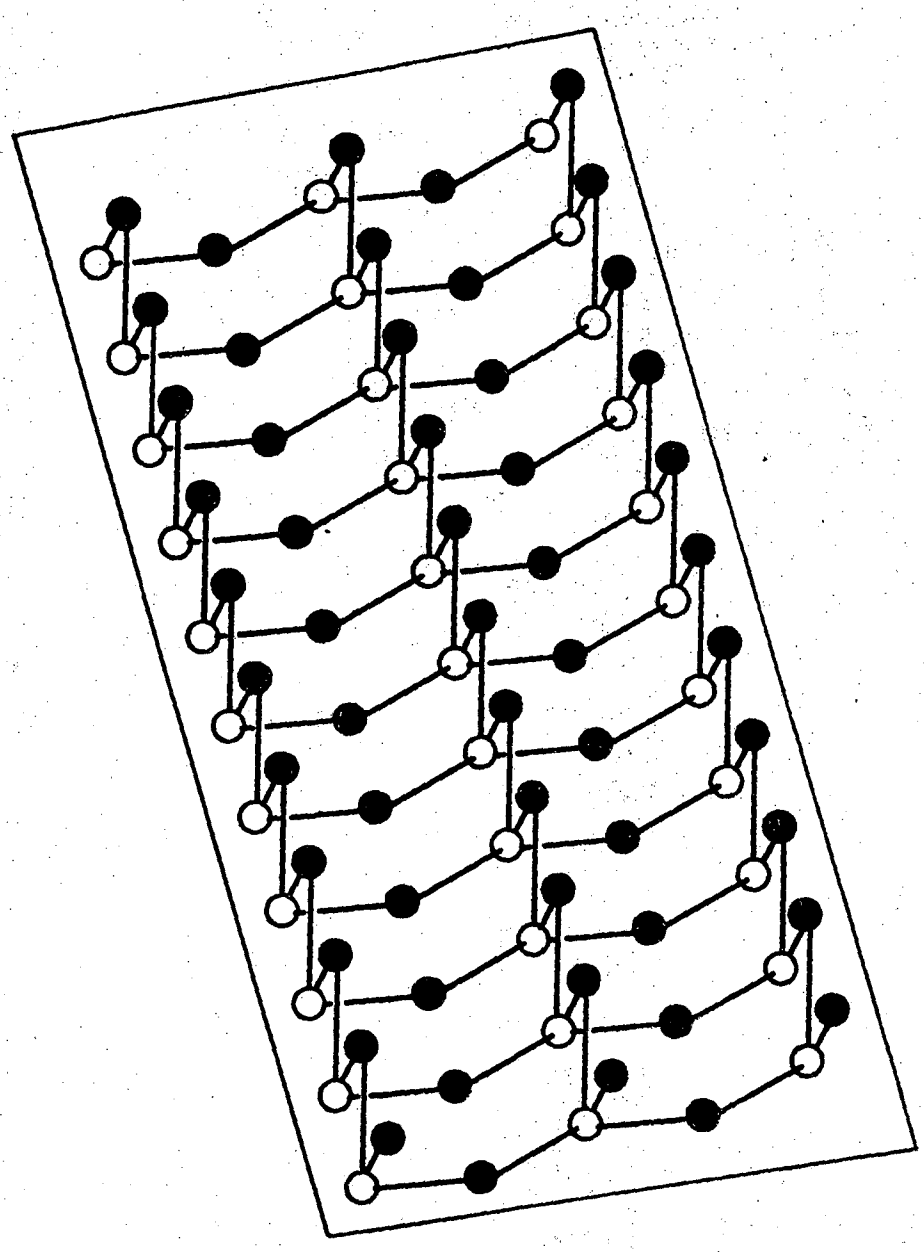

XBL 745-6224

Fig. 2.

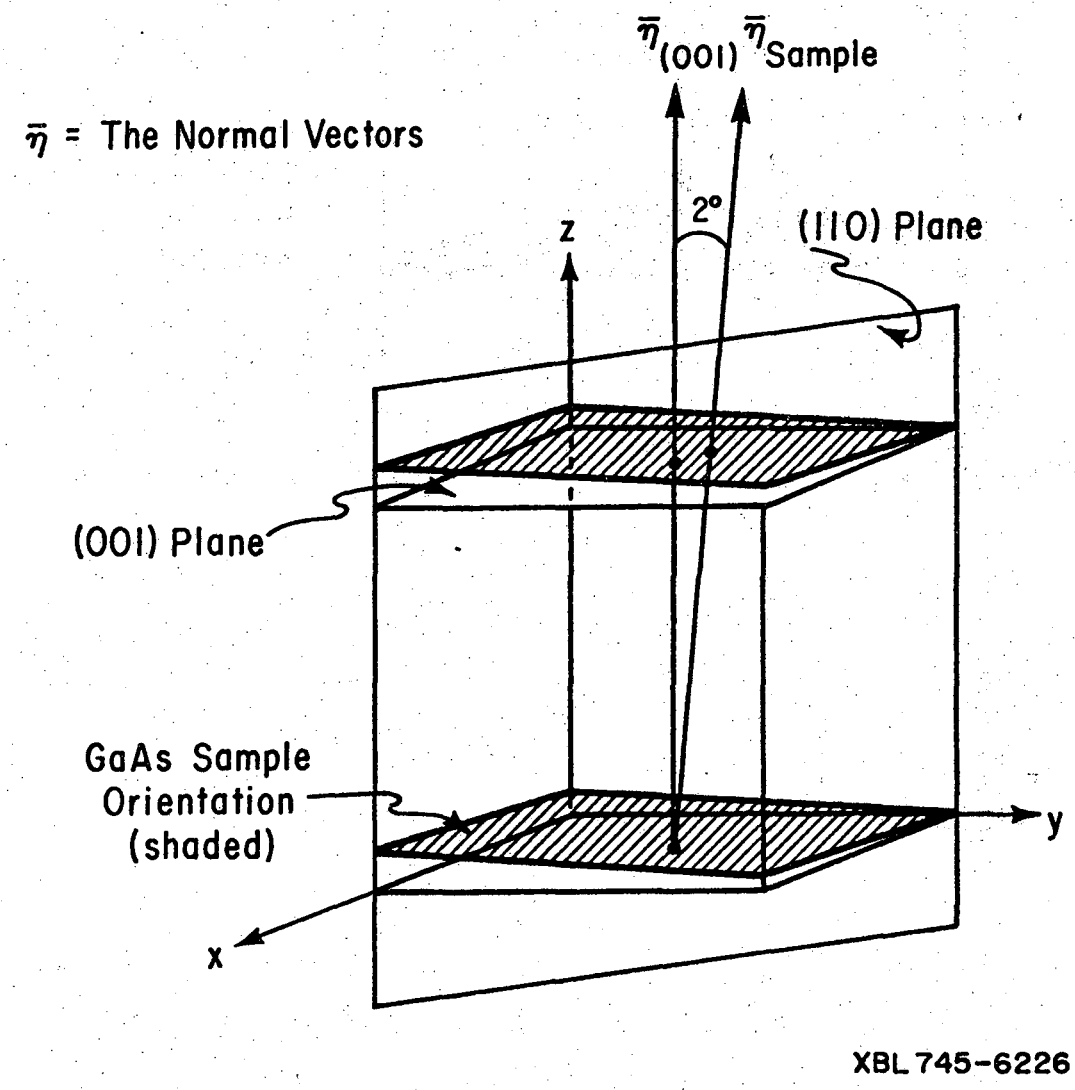
$\bar{\eta}_{(001)}$ $\bar{\eta}_{Sample}$
$\bar{\eta}$ = The Normal Vectors
2°
z
(110) Plane
(001) Plane
GaAs Sample
Orientation
(shaded)
y
x
XBL 745-6226

Fig. 3.

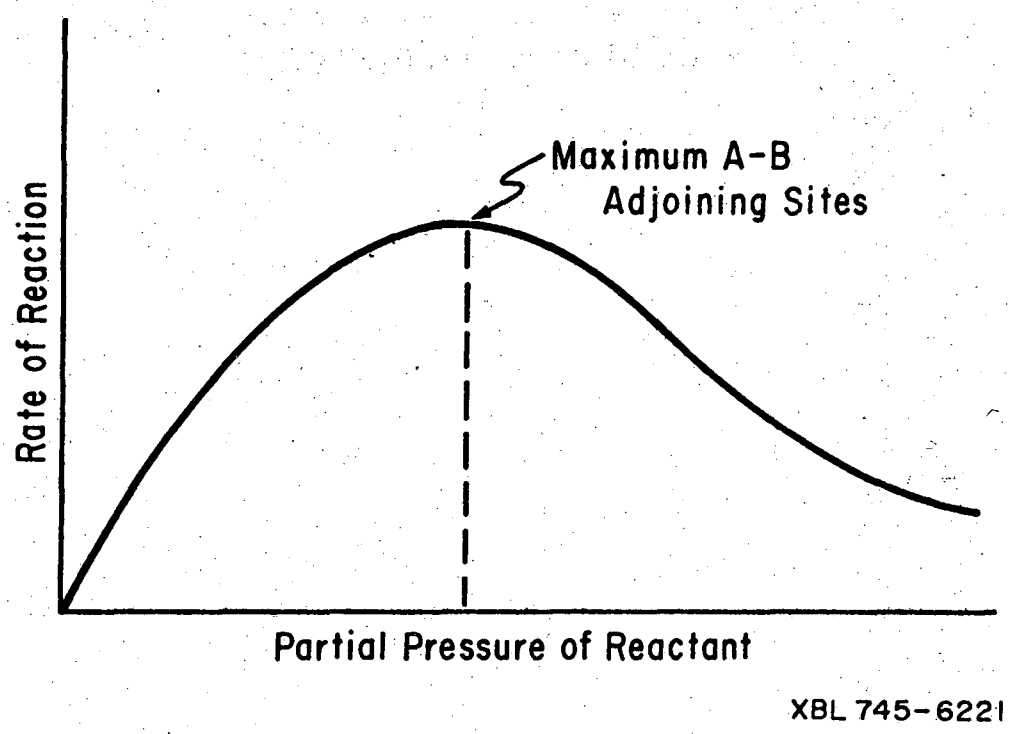
Maximum A-B
Adjoining Sites
Rate of Reaction
Partial Pressure of Reactant
XBL 745-6221

Fig. 4.

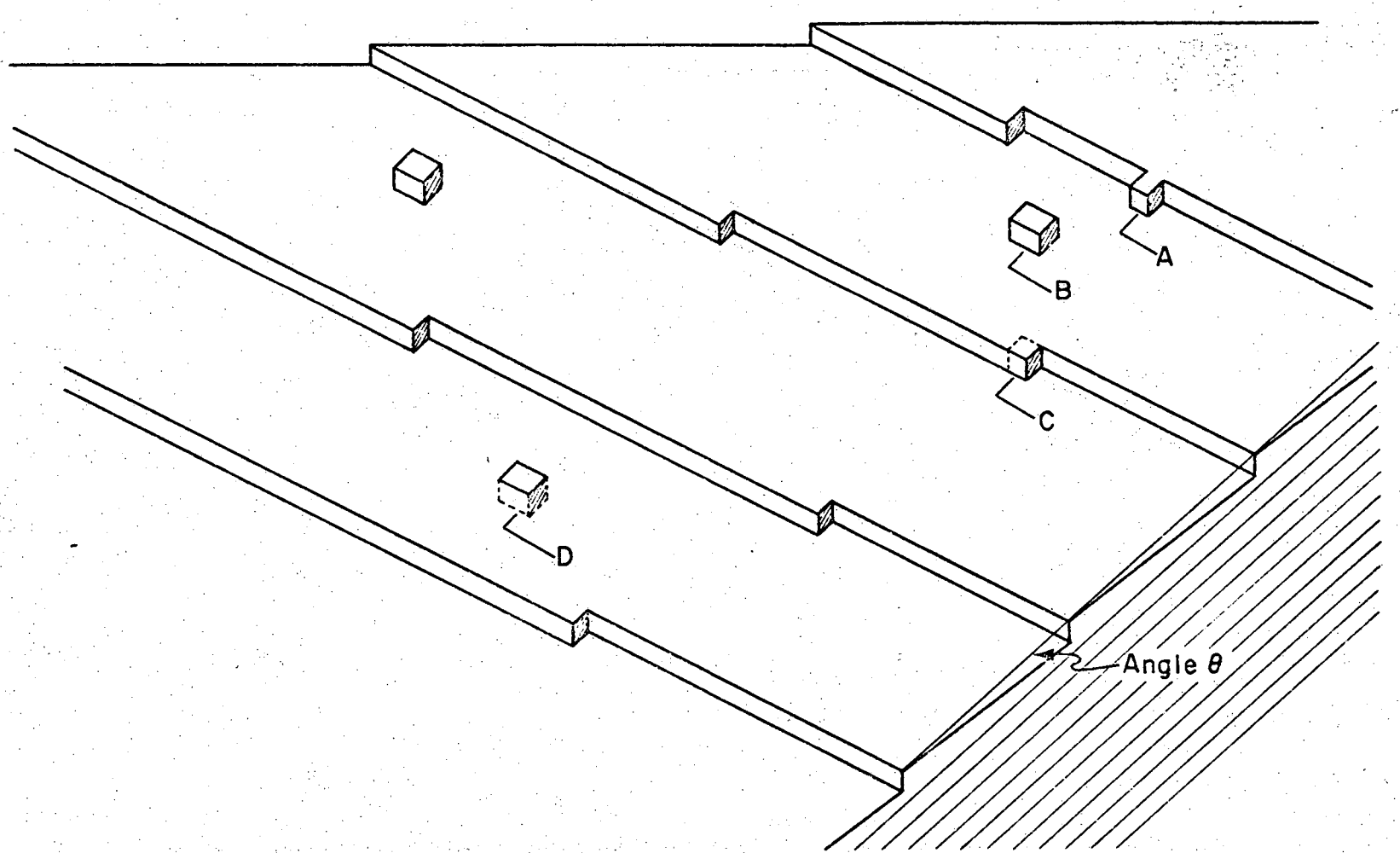

XBL 745-6269

Fig. 5.

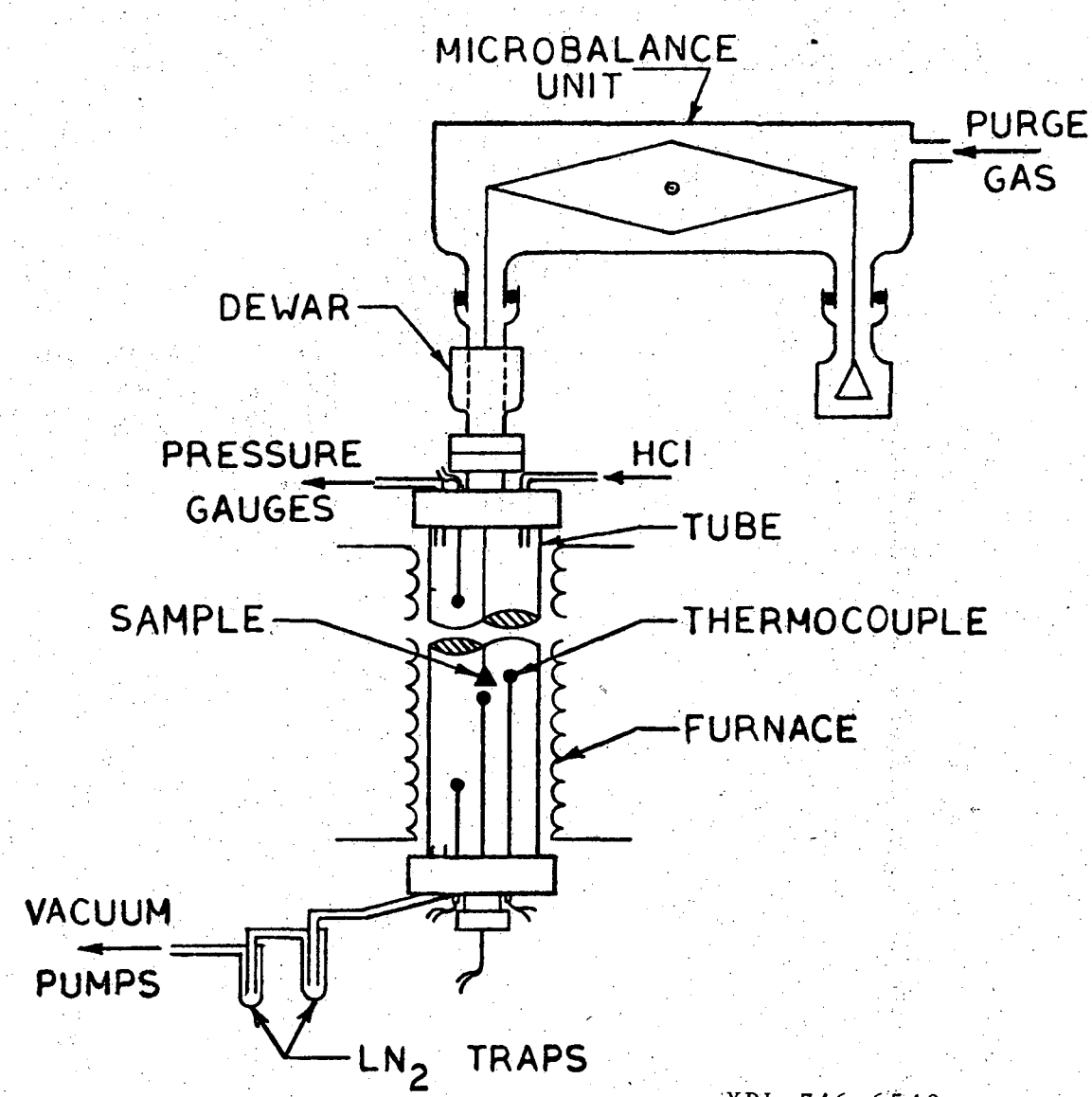

XBL 746-6540

Fig. 6.

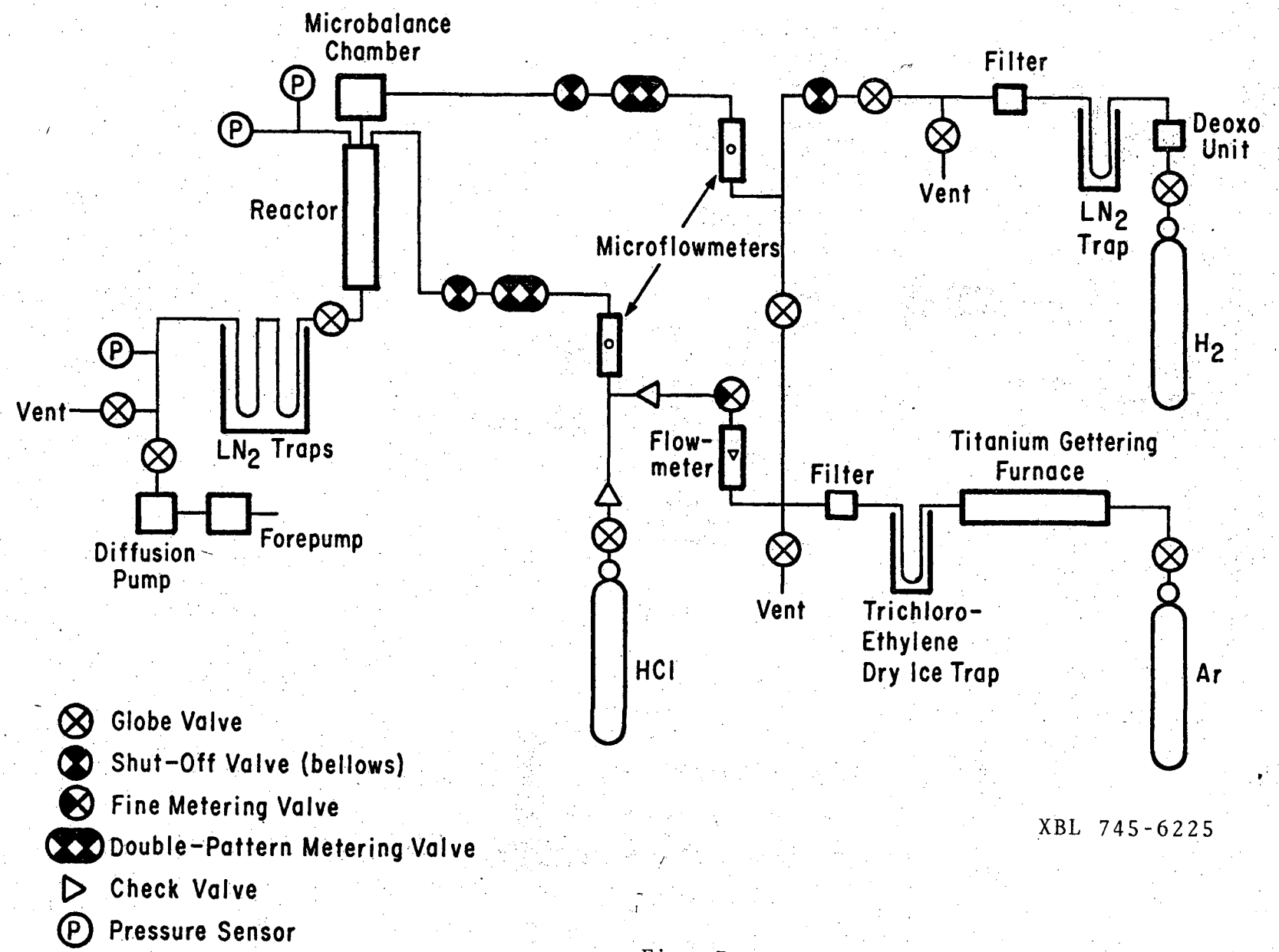

XBL 745-6225

Fig. 7.

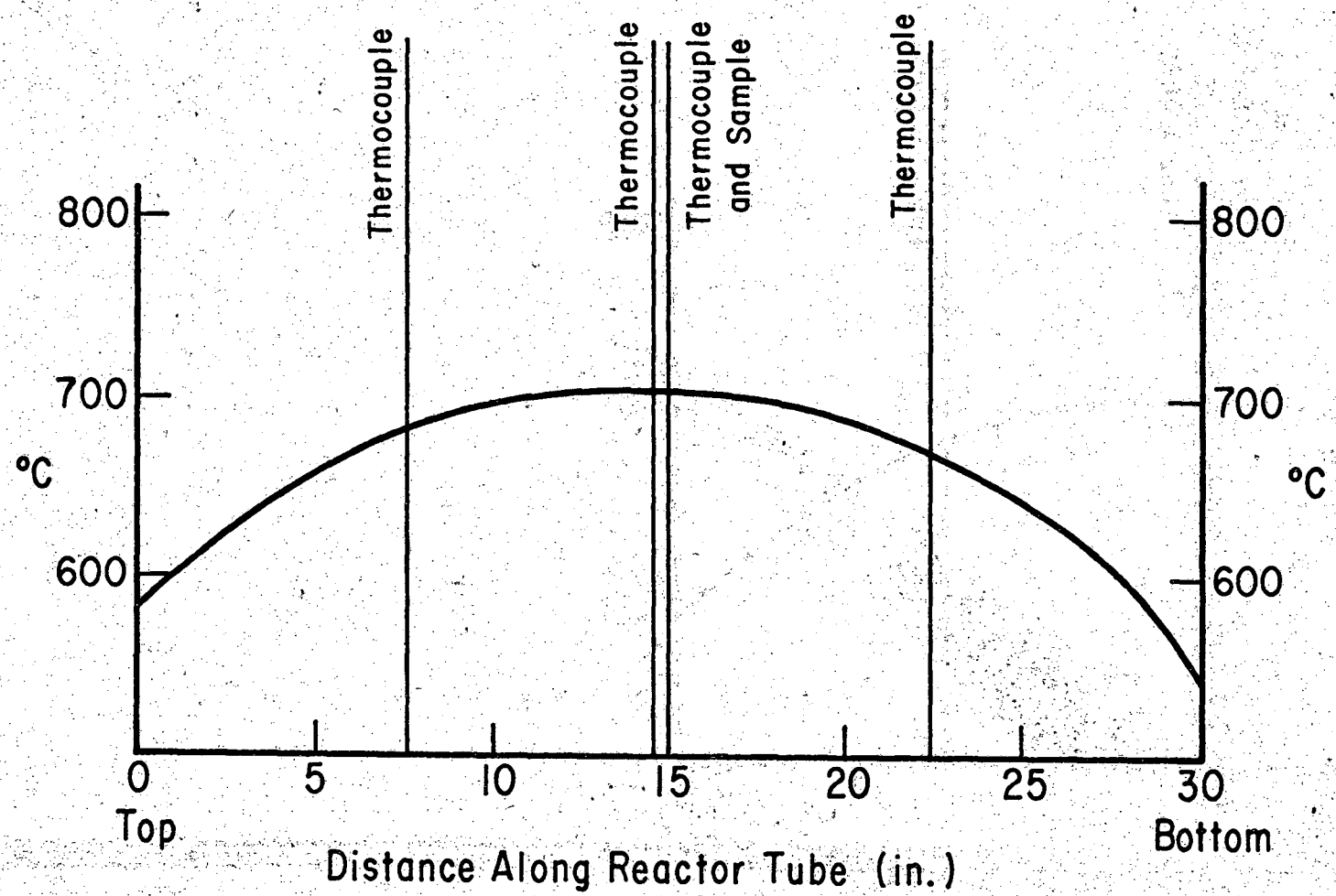

Fig. 8.

XBL 745-6222

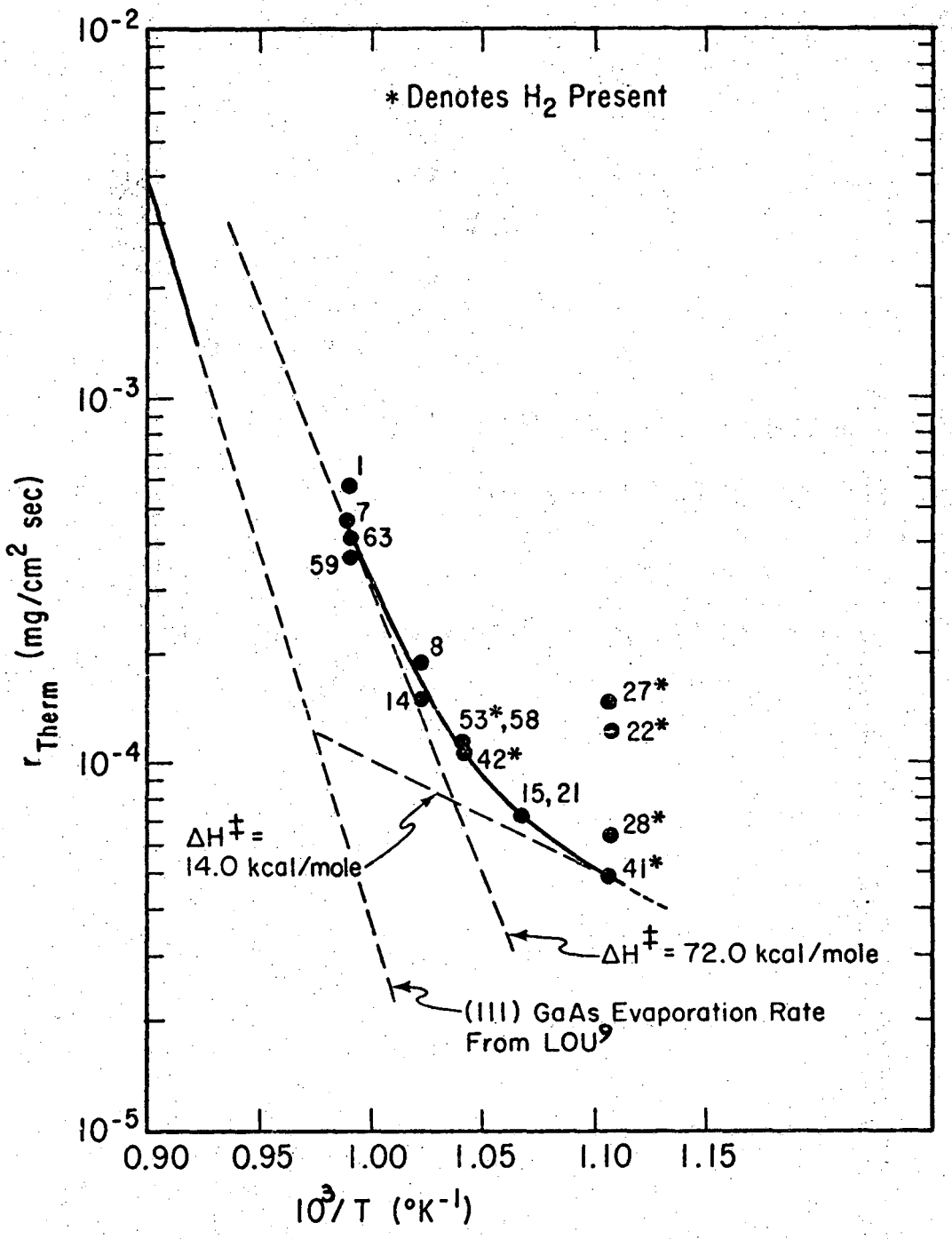

XBL 745-6211

Fig. 9.

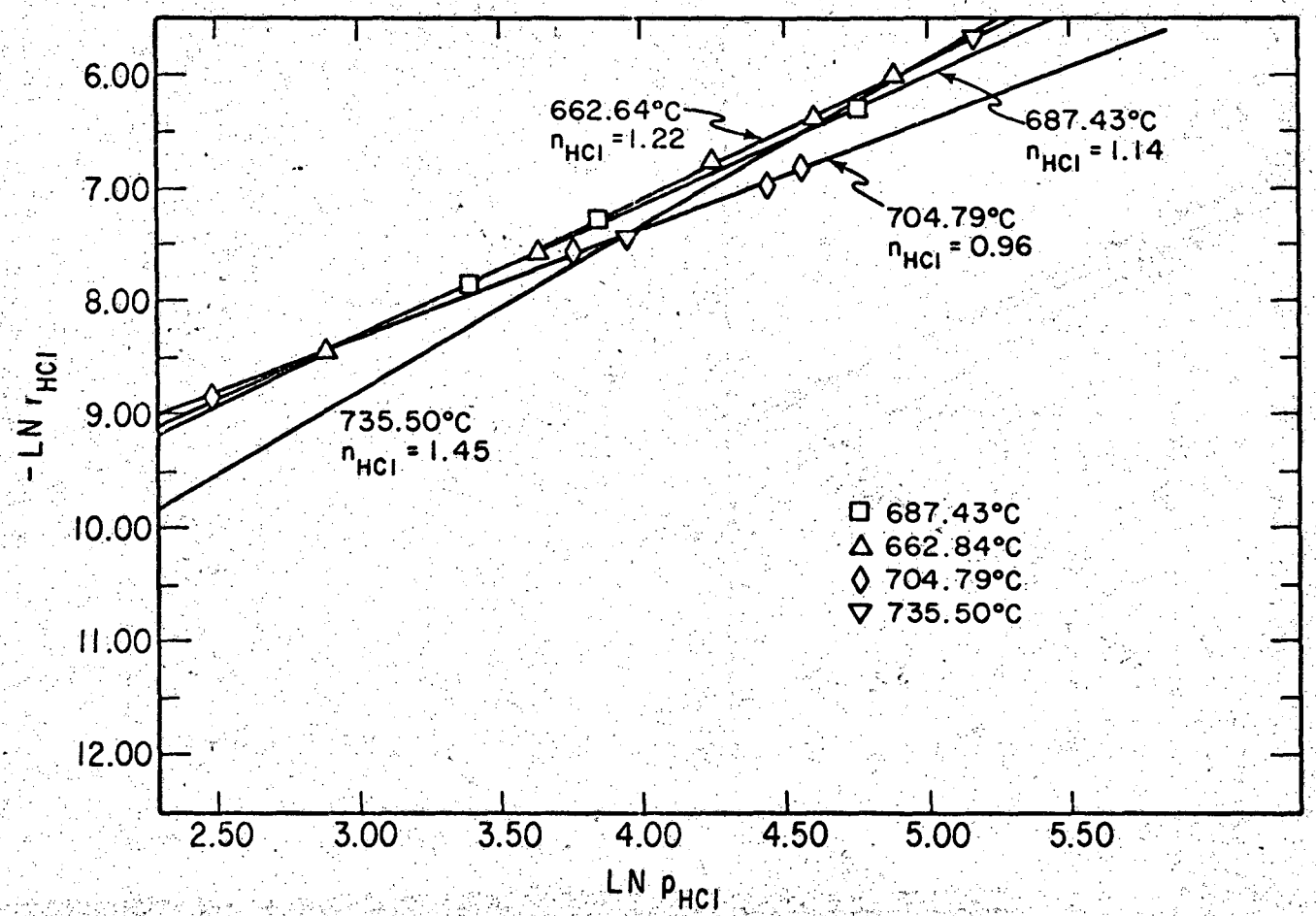

XBL 745-6217

Fig. 10.

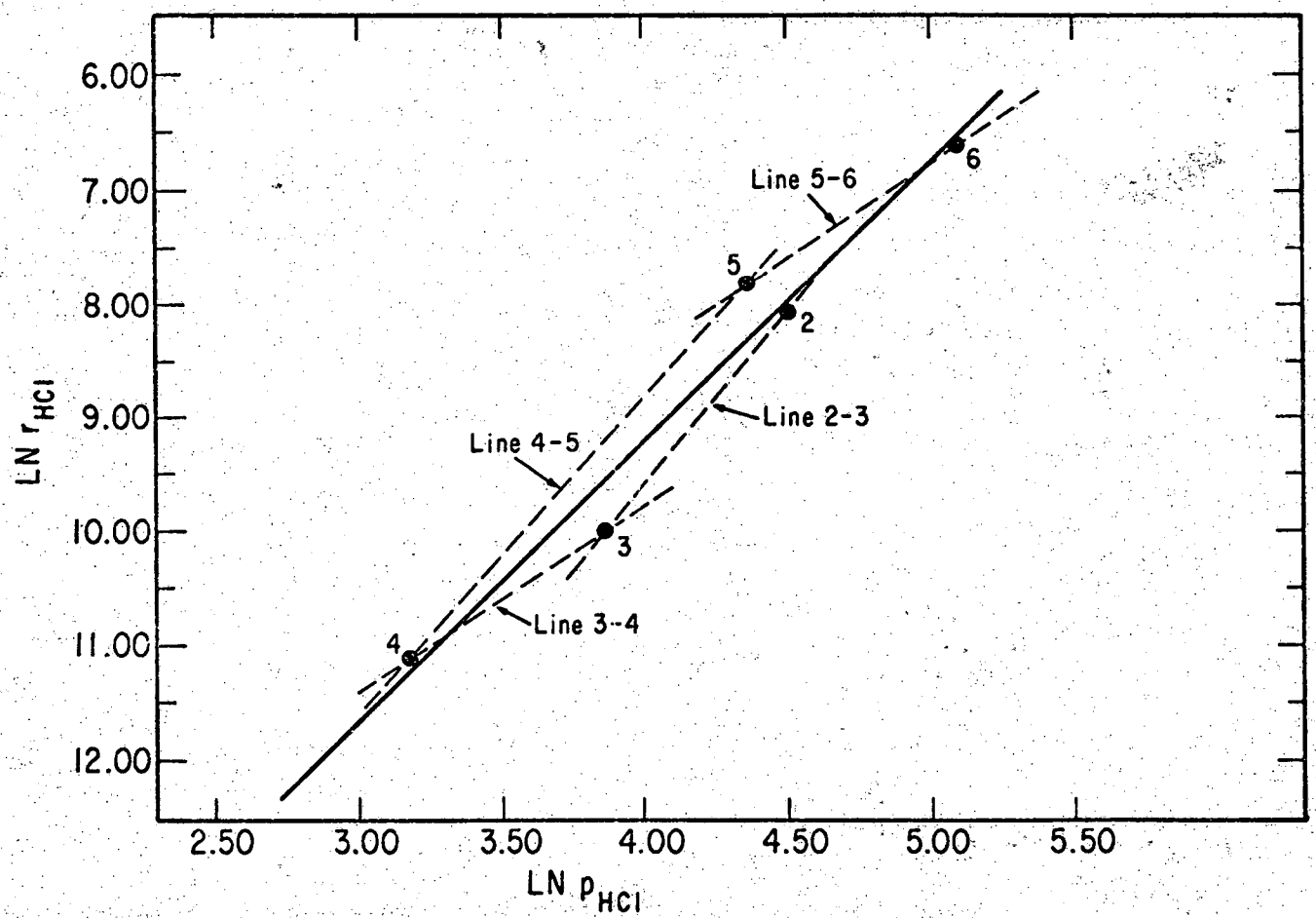

XBL 745-6213

Fig. 11.

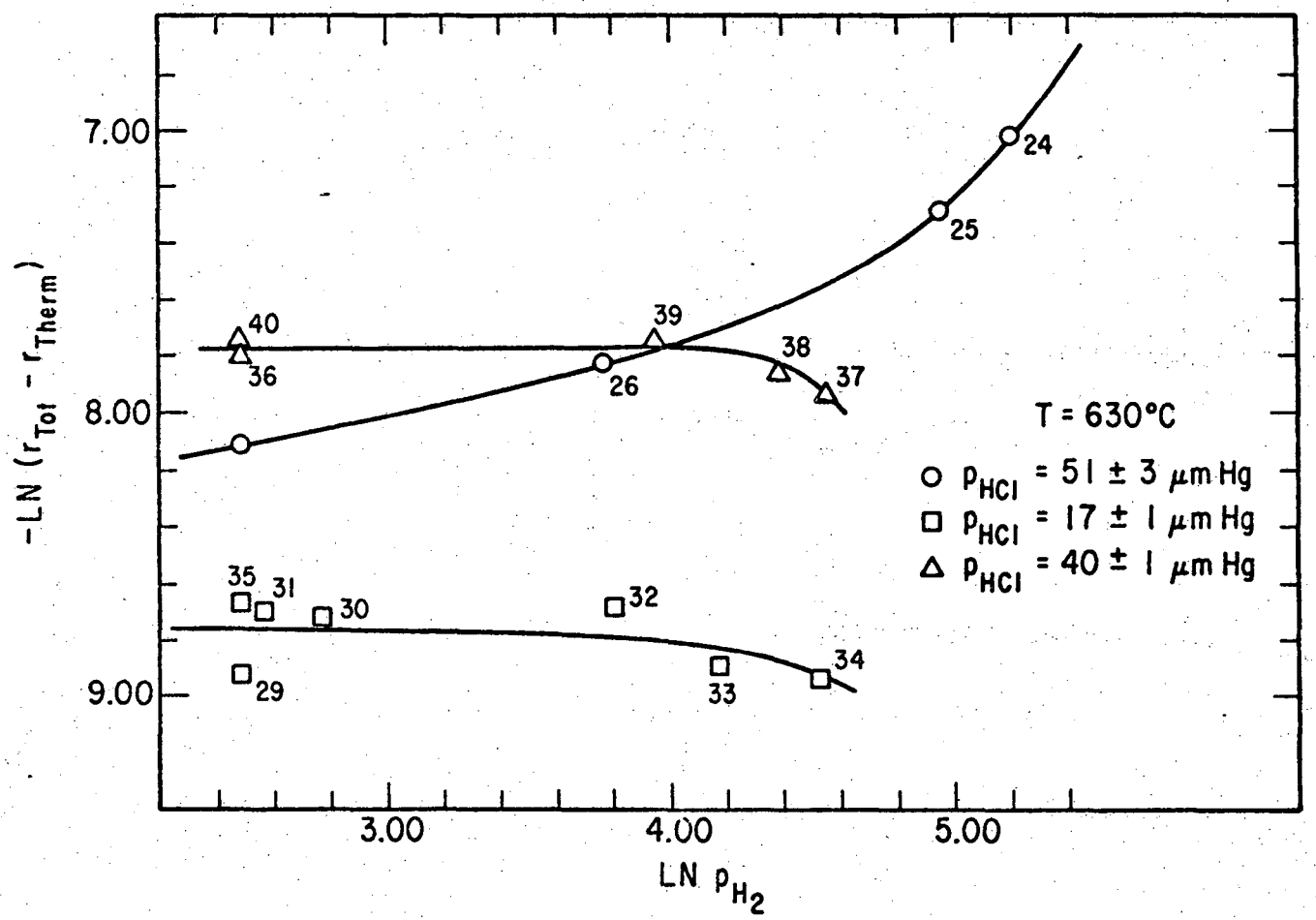

XBL 745-6214

Fig. 12.

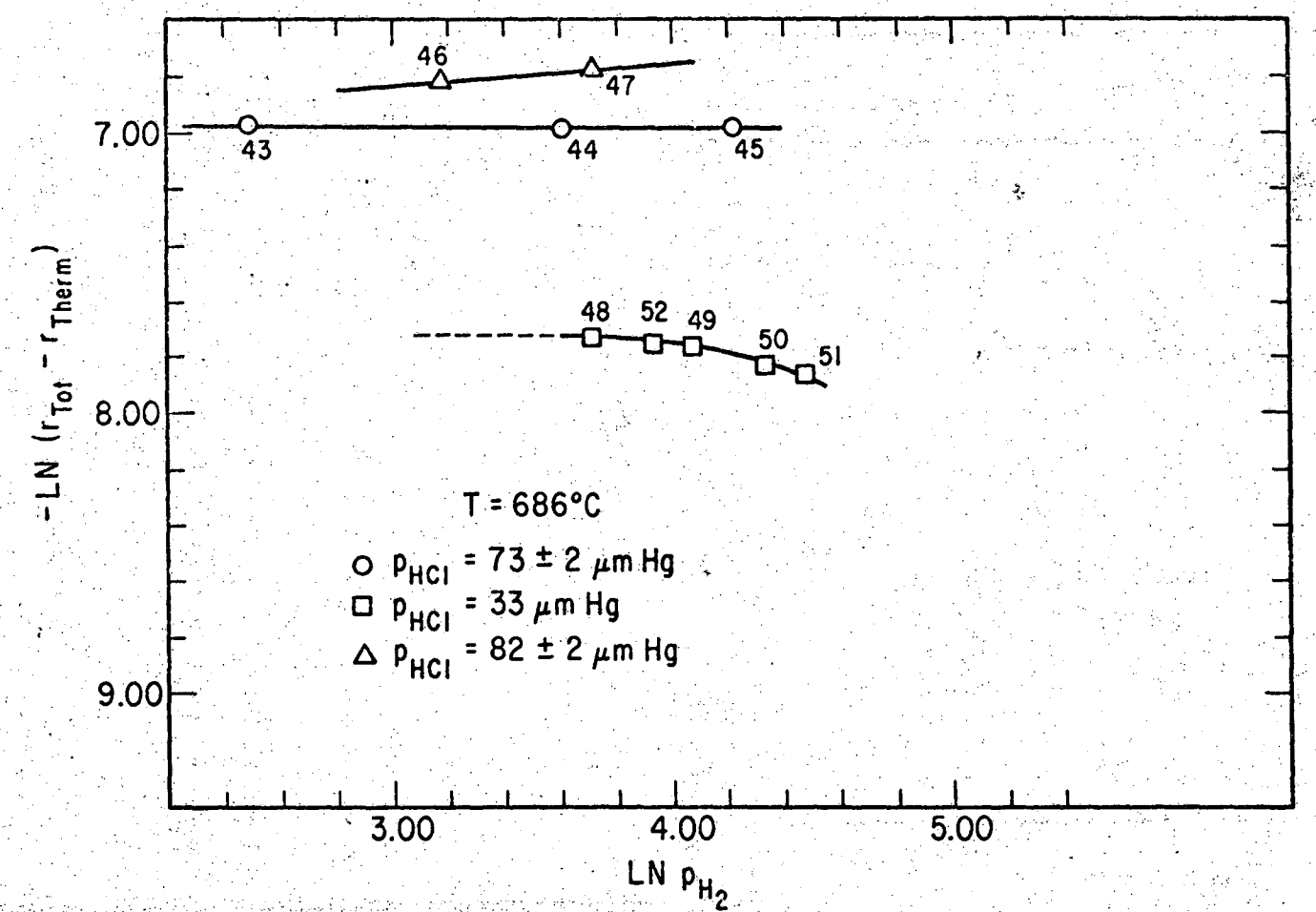

XBL 745-6215

Fig. 13.

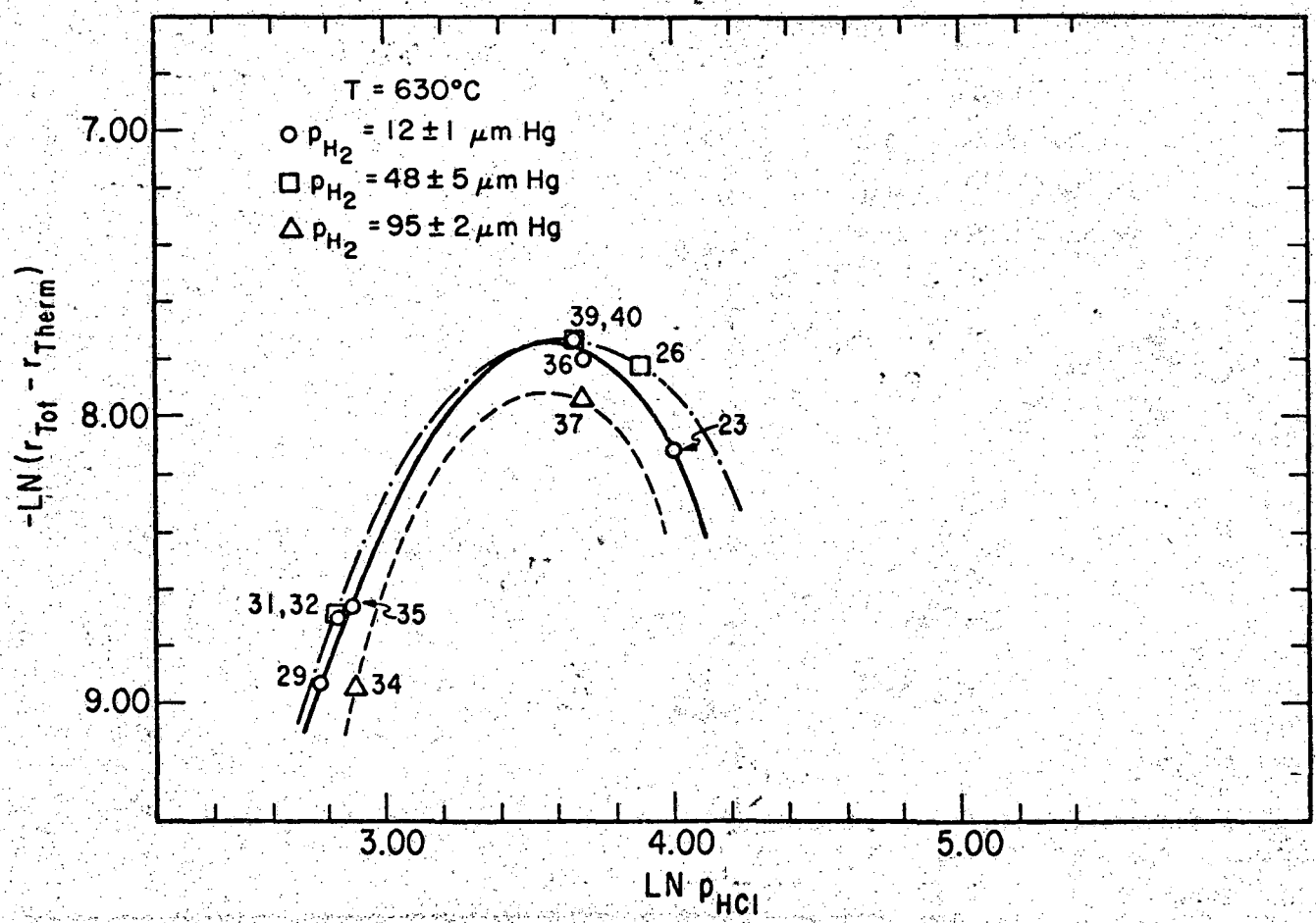

XBL 745-6212

Fig. 14.

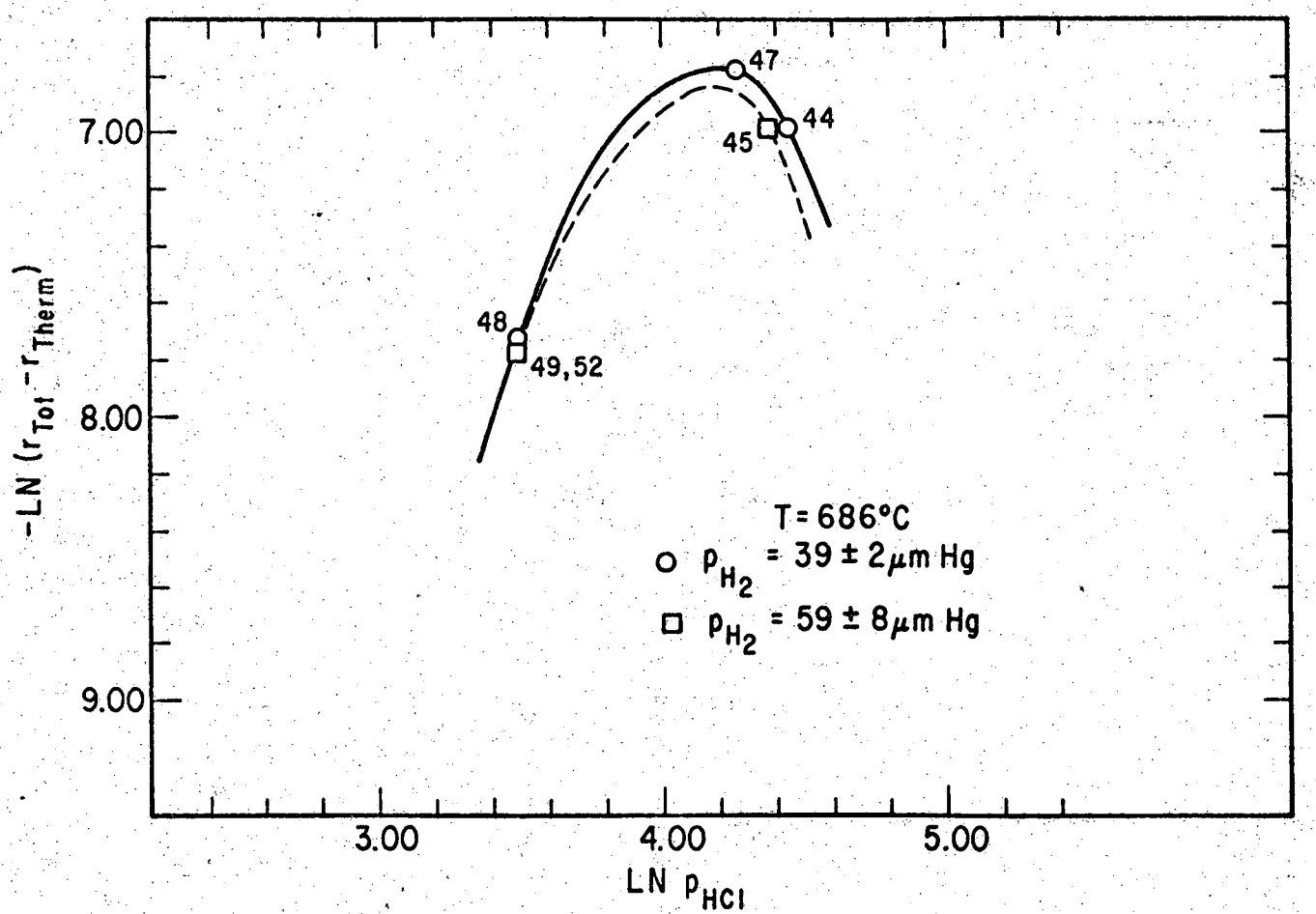

XBL 745-6218

Fig. 15.

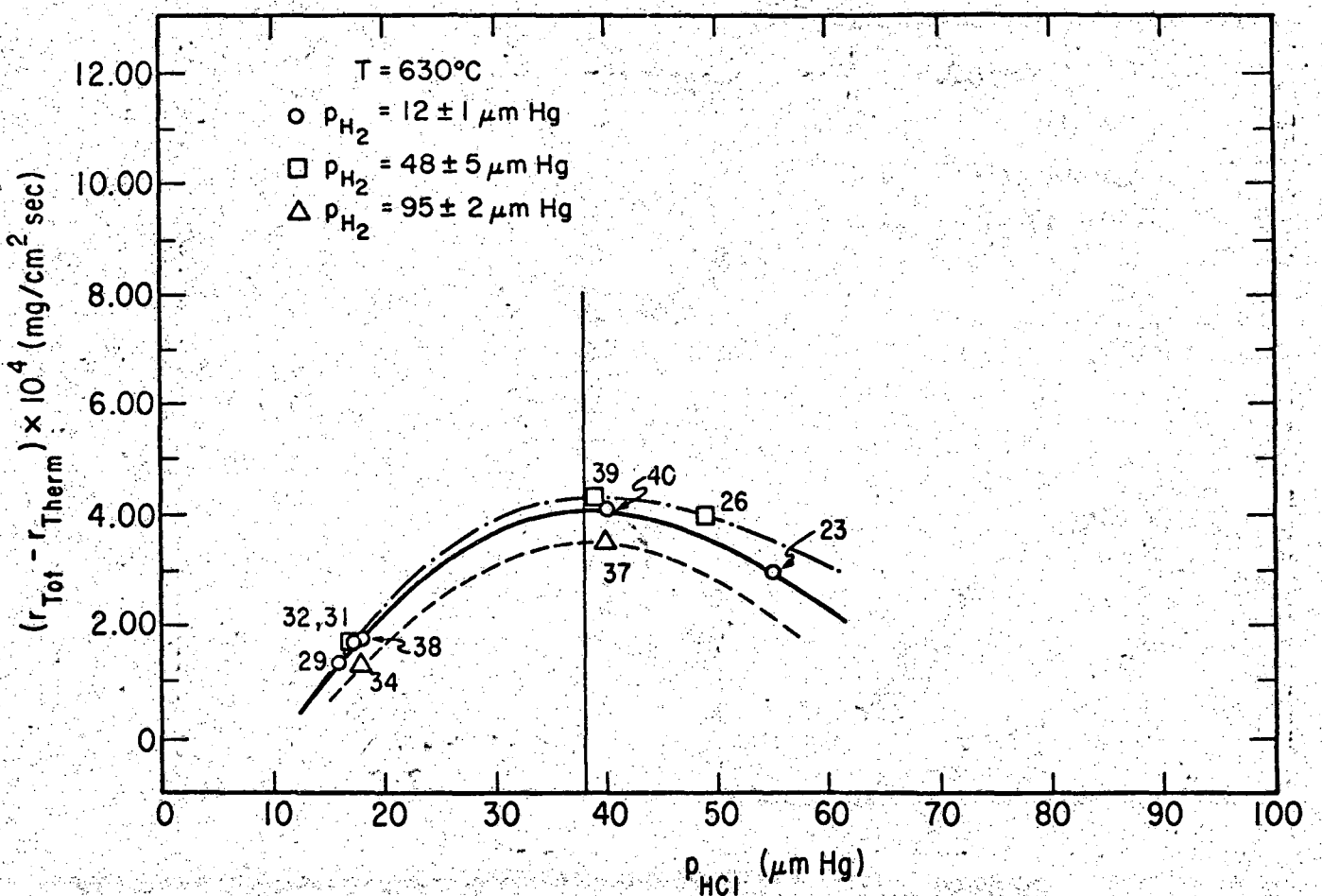

XBL 745-6216

Fig. 16.

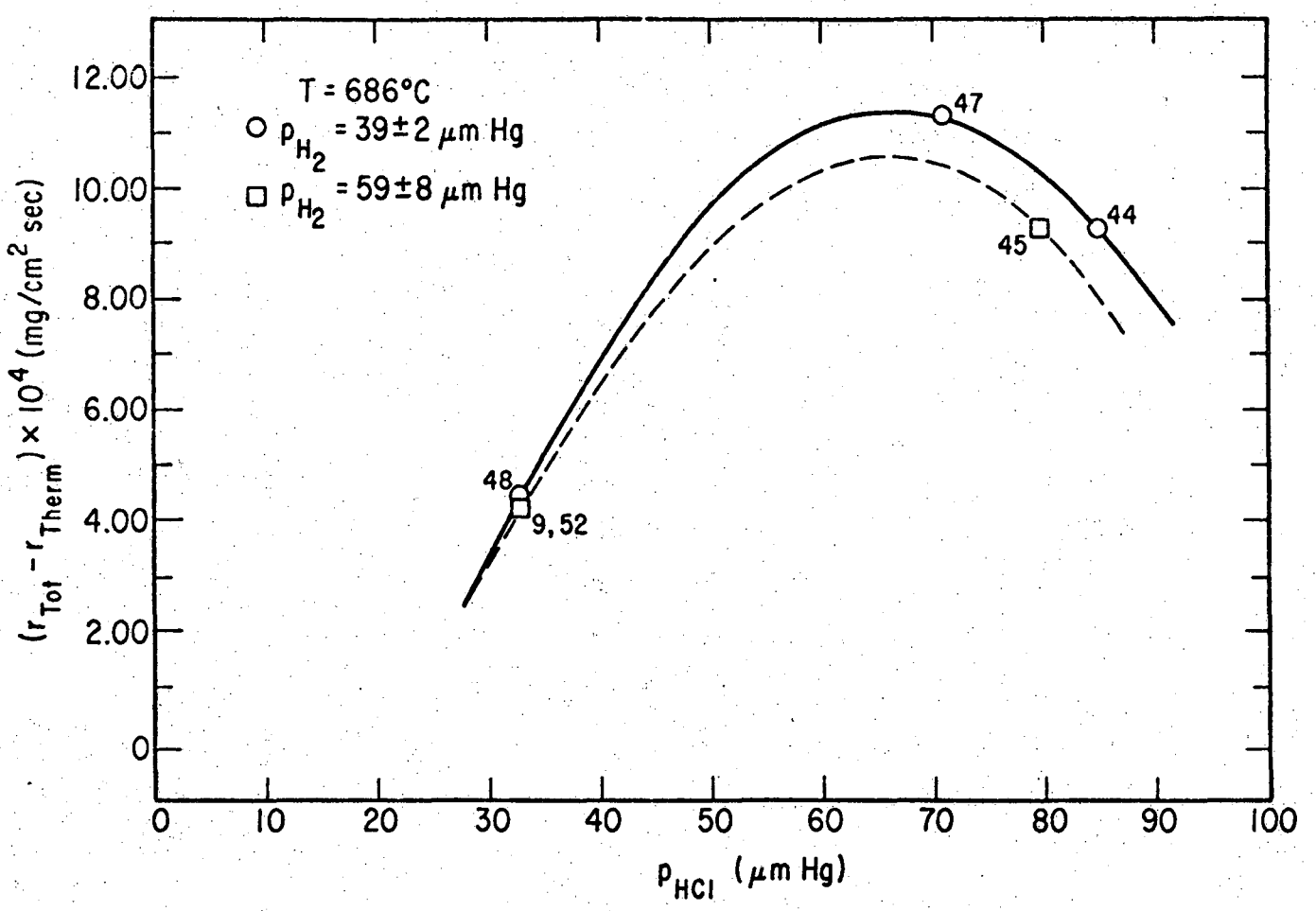

XBL 745-6209

Fig. 17.

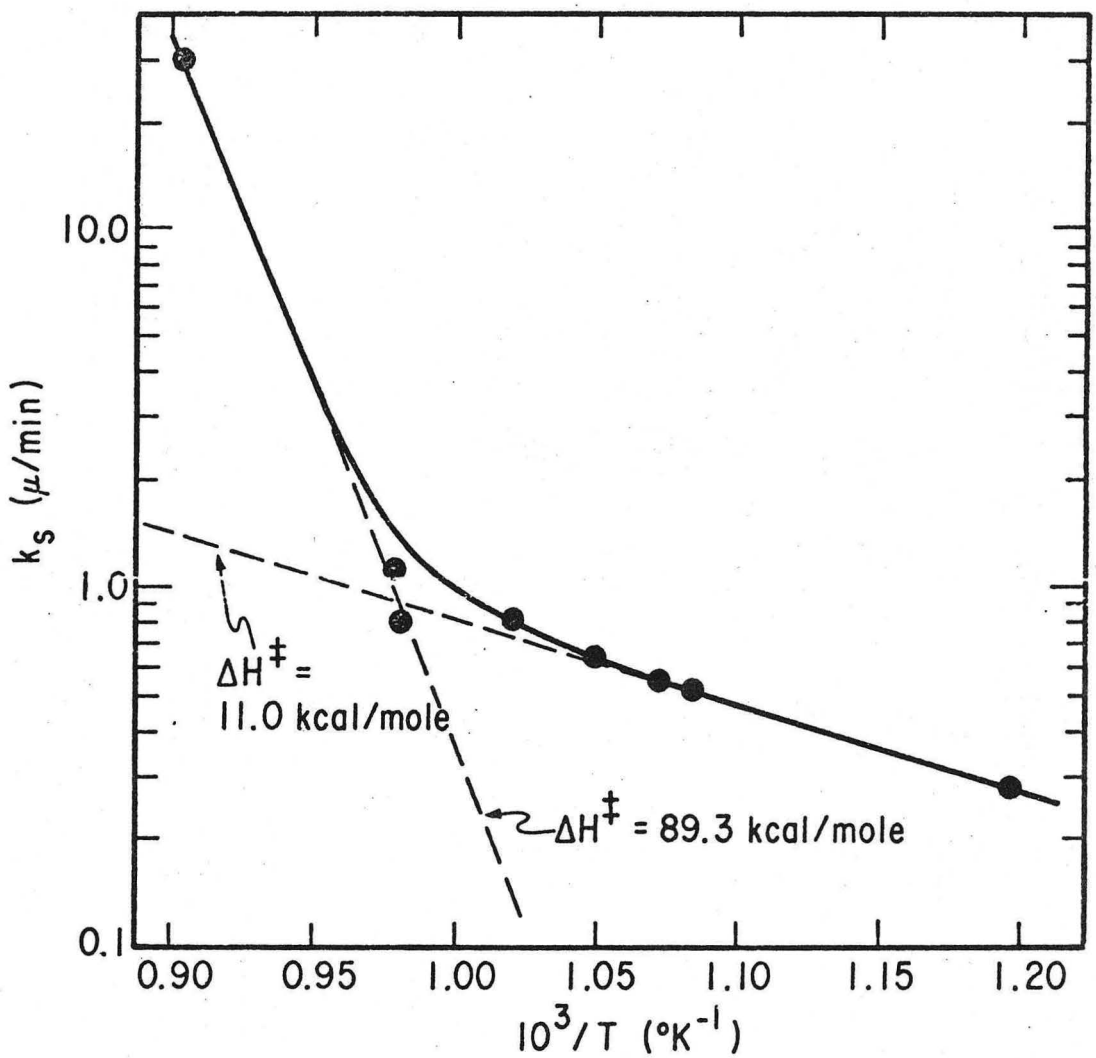

XBL745-6219

Fig. 18.

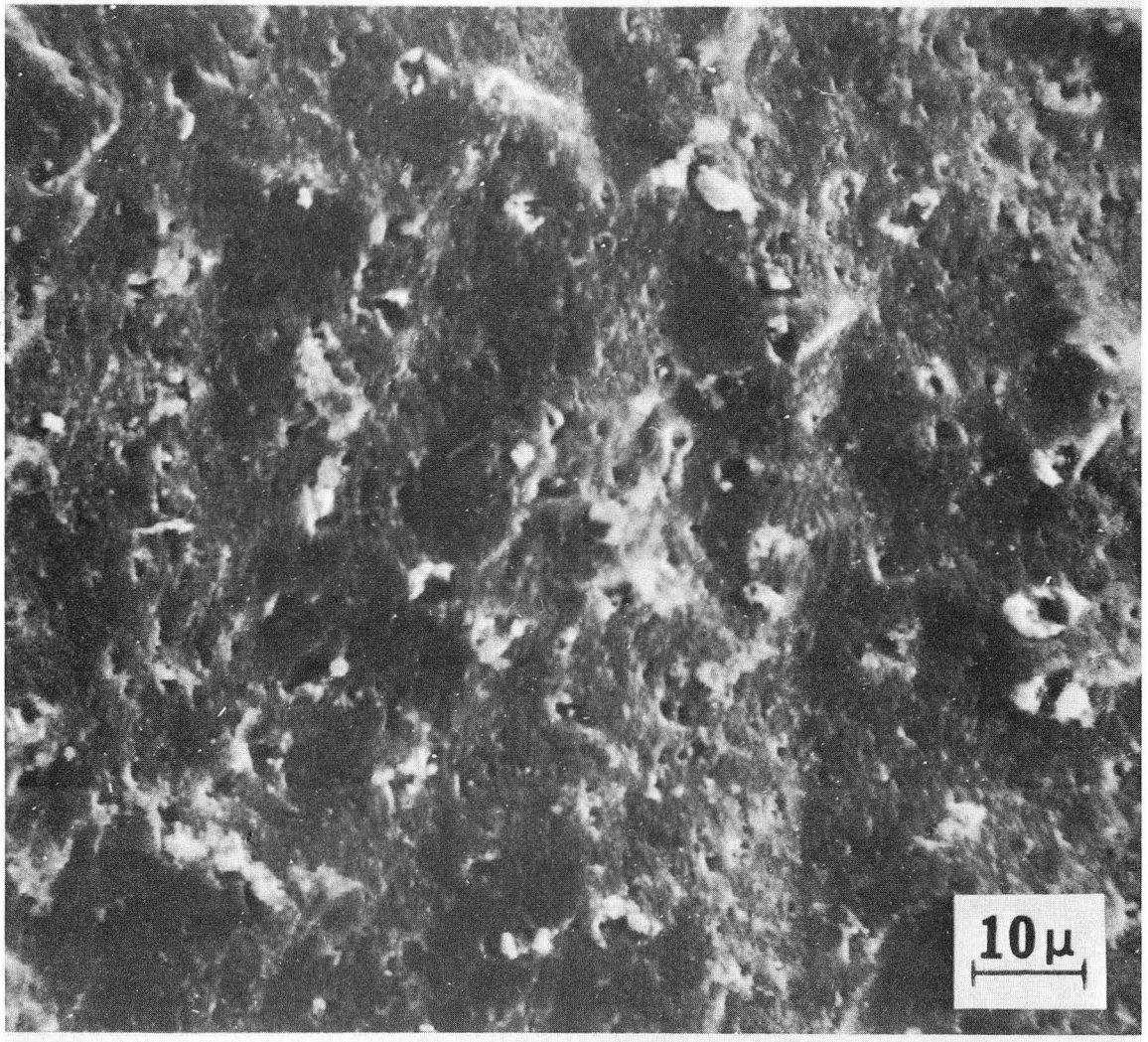

XBB 746-3796

Fig. 19.

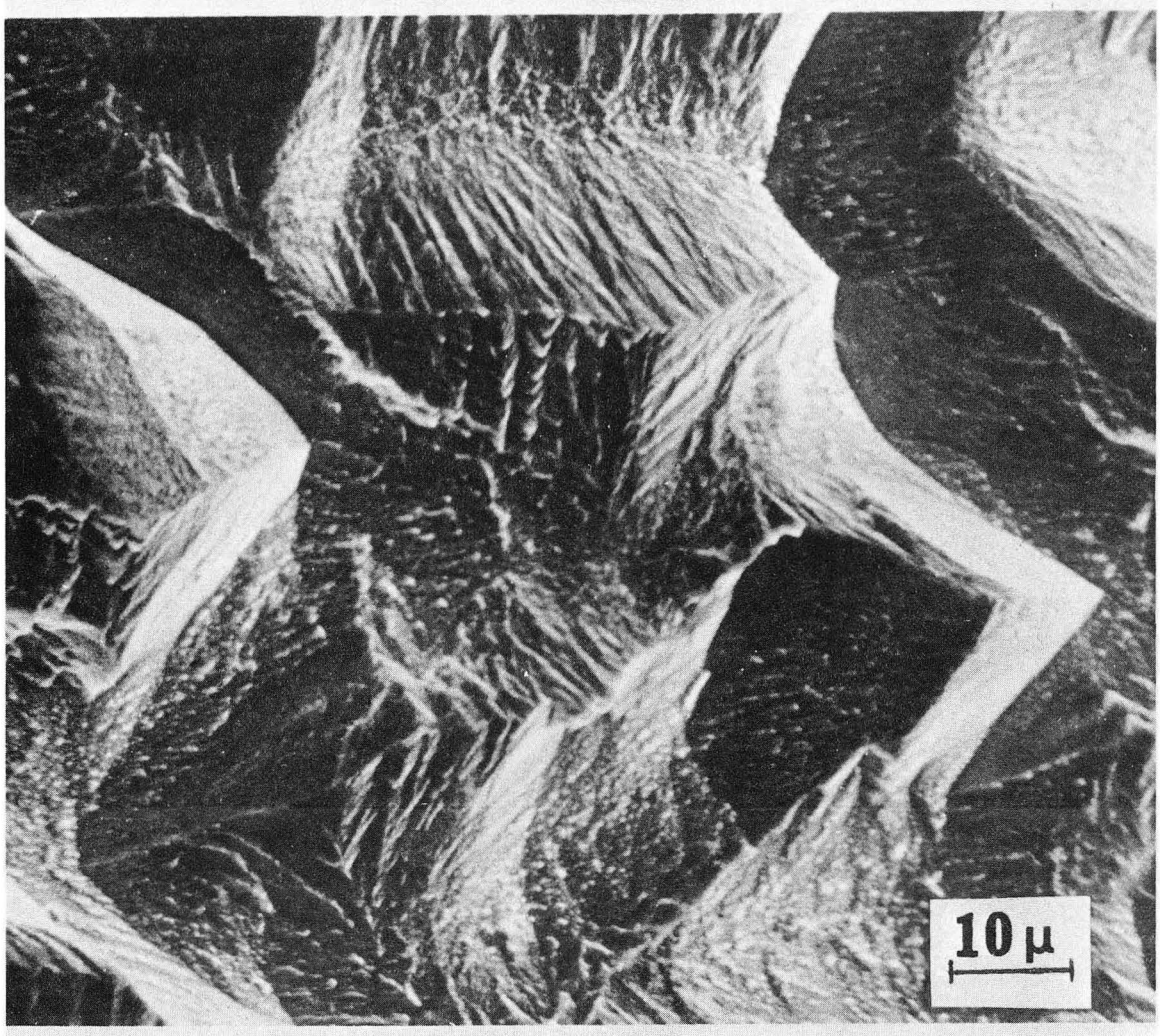

XBB 746-3800

Fig. 20.

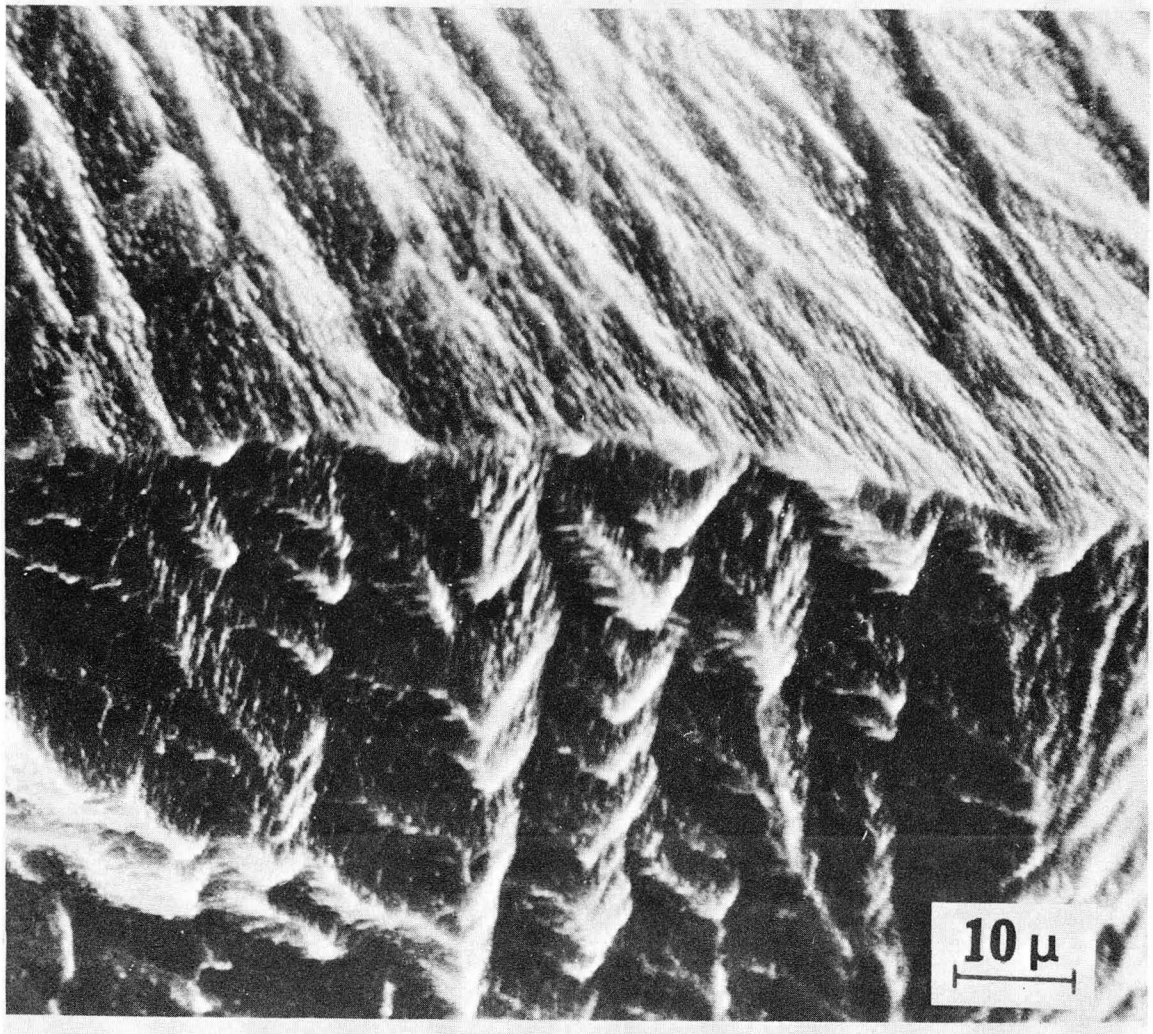

XBB 746-3798

Fig. 21.

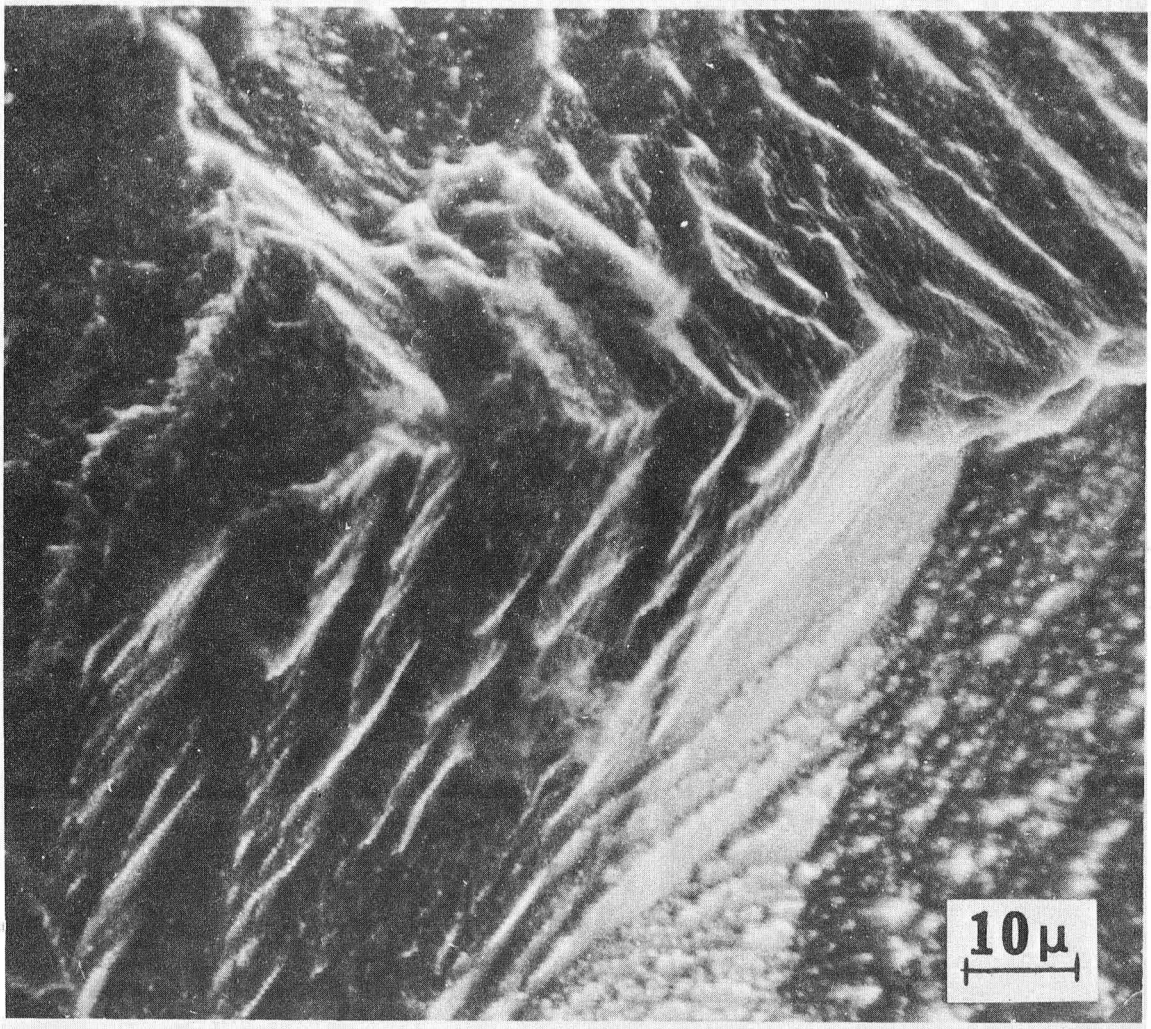

XBB 746-3797

Fig. 22.

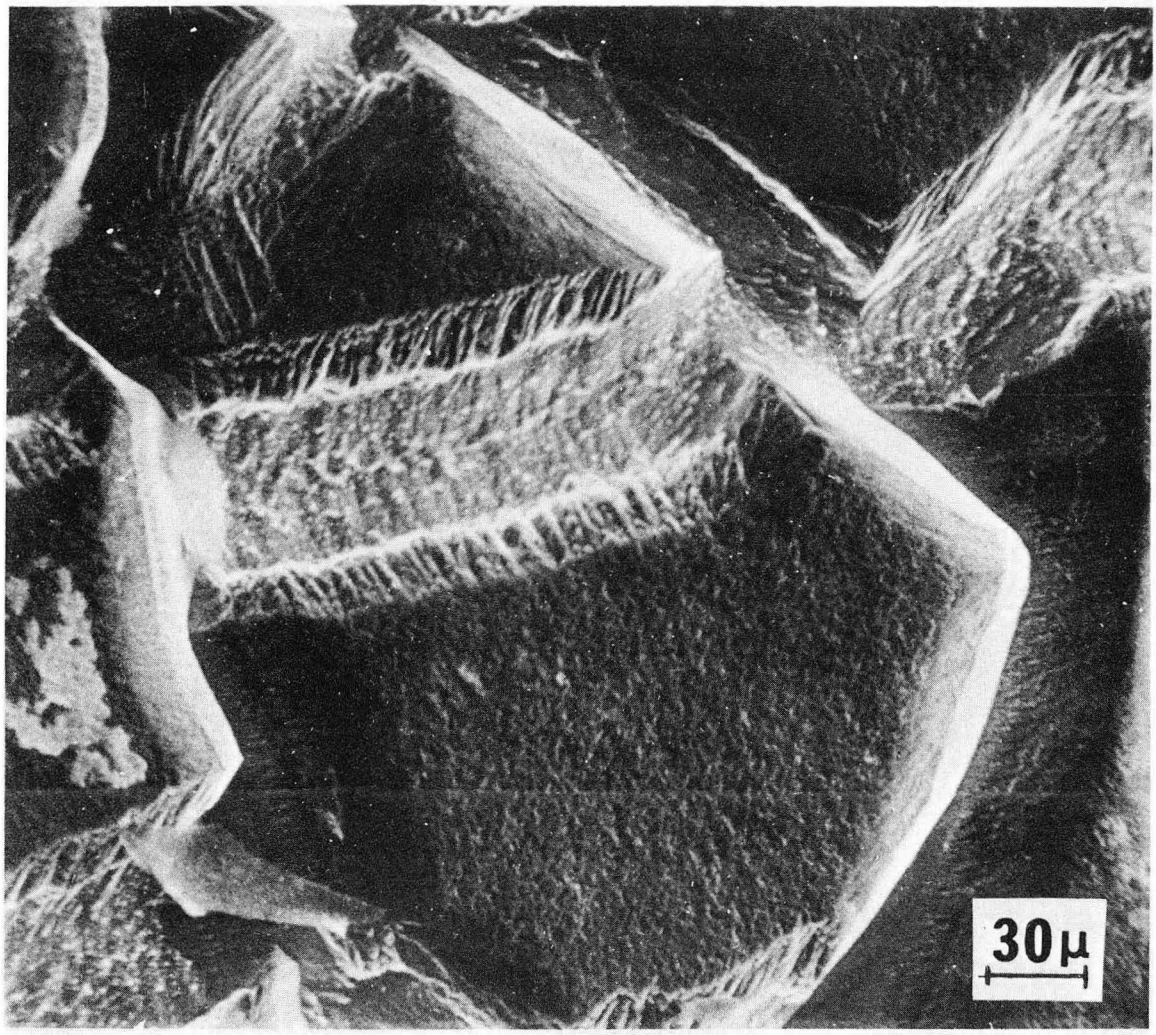

XBB 746-3801

Fig. 23.

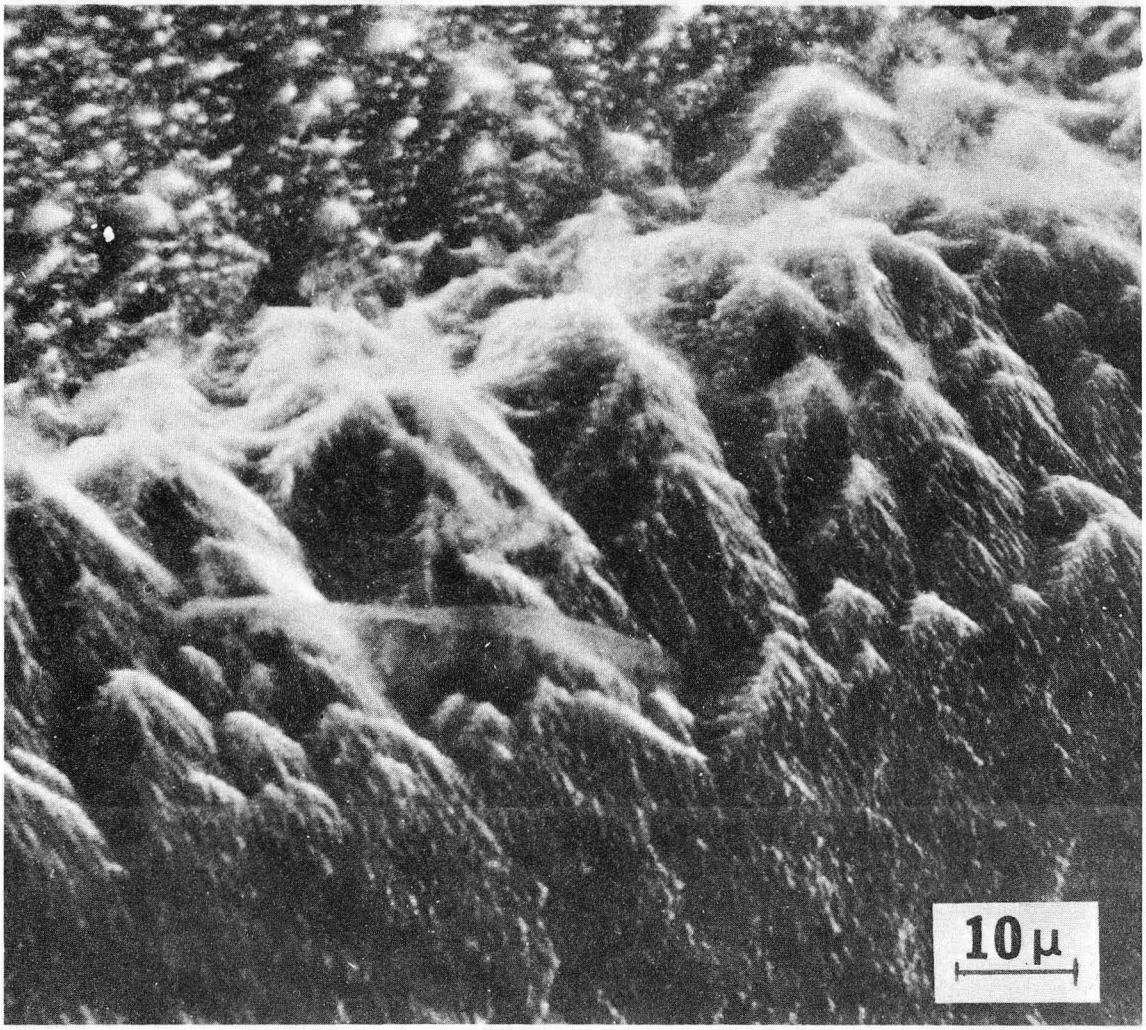

XBB 746-3799

Fig. 24.

LEGAL NOTICE

This report was prepared as an account of work sponsored by the United States Government. Neither the United States nor the United States Atomic Energy Commission, nor any of their employees, nor any of their contractors, subcontractors, or their employees, makes any warranty, express or implied, or assumes any legal liability or responsibility for the accuracy, completeness or usefulness of any information, apparatus, product or process disclosed, or represents that its use would not infringe privately owned rights.

TECHNICAL INFORMATION DIVISION
LAWRENCE BERKELEY LABORATORY
UNIVERSITY OF CALIFORNIA
BERKELEY, CALIFORNIA 94720